

# Accepted Manuscript

Design, synthesis and biological evaluation of novel  $\alpha$ -acyloxy carboxamides via Passerini reaction as caspase 3/7 activators

Mohammed Salah Ayoup, Yasmin Wahby, Hamida Abdel Hamid, El Sayed Ramadan, Mohamed Teleb, Marwa M. Abu-Serie, Ahmed Noby



PII: S0223-5234(19)30165-5

DOI: <https://doi.org/10.1016/j.ejmech.2019.02.051>

Reference: EJMECH 11143

To appear in: *European Journal of Medicinal Chemistry*

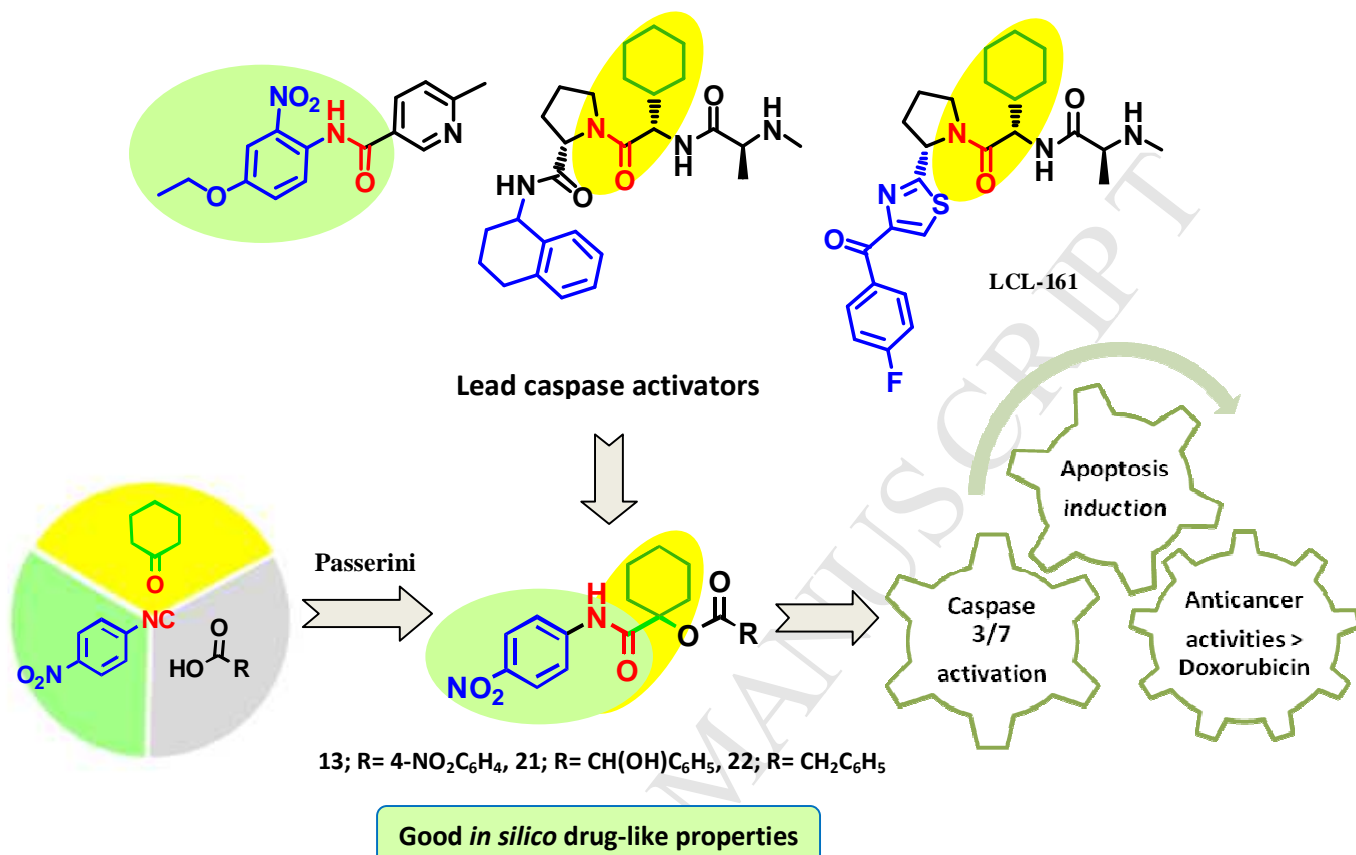
Received Date: 12 December 2018

Revised Date: 16 February 2019

Accepted Date: 17 February 2019

Please cite this article as: M. Salah Ayoup, Y. Wahby, H. Abdel Hamid, E.S. Ramadan, M. Teleb, M.M. Abu-Serie, A. Noby, Design, synthesis and biological evaluation of novel  $\alpha$ -acyloxy carboxamides via Passerini reaction as caspase 3/7 activators, *European Journal of Medicinal Chemistry* (2019), doi: <https://doi.org/10.1016/j.ejmech.2019.02.051>.

This is a PDF file of an unedited manuscript that has been accepted for publication. As a service to our customers we are providing this early version of the manuscript. The manuscript will undergo copyediting, typesetting, and review of the resulting proof before it is published in its final form. Please note that during the production process errors may be discovered which could affect the content, and all legal disclaimers that apply to the journal pertain.



ACCEPTED MANUSCRIPT

# Design, synthesis and biological evaluation of novel $\alpha$ -acyloxy carboxamides via Passerini reaction as caspase 3/7 activators

Mohammed Salah Ayoup<sup>a\*</sup>, Yasmin Wahby<sup>a</sup>, Hamida Abdel Hamid<sup>a</sup>, El Sayed Ramadan<sup>a</sup>, Mohamed Teleb<sup>b</sup>, Marwa M. Abu-Serie<sup>c</sup>, Ahmed Noby<sup>d</sup>

<sup>a</sup> Chemistry Department, Faculty of Science, Alexandria University, P.O. Box 426, Alexandria, Ibrahimia, 21321, Egypt.

<sup>b</sup> Department of Pharmaceutical Chemistry, Faculty of Pharmacy, Alexandria University, Alexandria 21521, Egypt.

<sup>c</sup> Medical Biotechnology Department, Genetic Engineering and Biotechnology Research Institute, City of Scientific Research and Technological Applications (SRTA-City), Egypt

<sup>d</sup> Department of Microbiology and Immunology, Faculty of Pharmacy, Pharos University in Alexandria, Alexandria 21311, Egypt.

\* Corresponding author at: Chemistry Department, Faculty of Science, Alexandria University, P.O. Box 426, Alexandria, Ibrahimia, 21321, Egypt

Email address: [mohammedsalahayoup@gmail.com](mailto:mohammedsalahayoup@gmail.com)

[Mohamed.salah@alexu.edu.eg](mailto:Mohamed.salah@alexu.edu.eg)

## Abstract

Evasion of apoptosis is a hallmark of cancer. Caspases; the key executors of apoptotic cascade are attractive targets for selective induction of apoptosis in cancer cells. Within this approach, various caspase activators were introduced as lead anticancer agents. In the current study, a new series of multifunctional Passerini products was synthesized and evaluated as potent caspase-dependent apoptotic inducers. The synthetic strategy adopted this isocyanide-based multicomponent reaction to possibly mimic the pharmacophoric features of various lead apoptotic inducers, where a series of  $\alpha$ -acyloxy carboxamides was prepared from *p*-nitrophenyl isonitrile, cyclohexanone and various carboxylic acids. Accordingly, the main amide-based scaffold was decorated by substituents with varying nature and size to gain more information about structure-activity relationship. All the synthesized compounds were screened for cytotoxicity against normal human fibroblasts and their potential anticancer activities against three human cancer cell lines; MCF-7 (breast), NFS-60 (myeloid leukemia), and HepG-2 (liver) utilizing MTT assay. Among the most active compounds, **13**, **21** and **22** were more potent and safer than doxorubicin with nanomolar IC<sub>50</sub> values and promising selectivity indices. Mechanistically, **13**, **21** and **22** induced apoptosis by significant caspase activation in all the screened cancer cell lines utilizing flow cytometric analysis and caspase 3/7 activation assay. Again, **13** and **21** recorded higher activation percentages than doxorubicin, while **22** showed comparable results. Apoptosis-inducing factor1 (AIF1) quantification assay declared that **13**, **21** and **22** didn't mediate apoptosis through AIF1-dependent pathway (i.e. only by caspase activation). Physicochemical properties, pharmacokinetic profiles, ligand efficiency metrics and drug-likeness data of all the synthesized compounds were computationally predicted and showed that **13**, **21** and **22** could be considered as drug-like candidates. Finally, selected compounds were preliminarily screened for possible antimicrobial activities searching for dual anticancer/antimicrobial agents as an advantageous approach for cancer therapy.

**Keywords:** Passerini; caspase 3/7 activator; anticancer; apoptotic inducer

## 1. Introduction

In 2017, the World Health Organization passed the resolution “*Cancer Prevention and Control through an Integrated Approach*” recognizing cancer as a leading cause of morbidity globally, accounting for about 9.6 million deaths in its up-to-date statistics [1]. The estimated annual number of new cancer cases projected to increase from 14.1 million in 2012 to 21.6 million by 2030 [2]. In recognition of the burden posed by cancer as a growing public health problem, extensive studies have been conducted to investigate various cancer mechanisms [3] and possible treatment strategies [4]. Within this context, abnormal apoptosis is considered as a hallmark in carcinogenesis and a popular target of many anticancer agents [5,6]. Apoptosis is the normal programmed cell death process that organisms use to maintain tissue homeostasis [7]. The mechanism underlying apoptosis is essentially controlled by a cascade of initiator and effector caspases that are sequentially activated. Caspases are a family of cysteinyl-aspartate-specific proteases that cleave an aspartic acid residue from their respective peptide substrates in the presence of a histidine residue [8,9]. This property irreversibly leads to cell death. Among these caspases, caspases-3 and -7 are believed to be the key effectors of the apoptotic pathway whose activities are critical for the execution of apoptosis [10–12]. It is worth mentioning that in addition to the classical caspase-dependent apoptosis, cells can undergo caspase-independent apoptosis by releasing the apoptosis-inducing factor1 (AIF1), which translocates to the nucleus for disrupting the nuclear chromatin [13].

Along these lines, apoptotic caspases are considered as attractive targets for selective induction of apoptosis in cancer cells [14]. Literature survey revealed various anticancer lead compounds that efficiently trigger apoptosis by different caspase-mediated mechanisms [15]. A series of substituted *N*-(2-nitrophenyl)nicotinamides **I** (**Fig.1**) has been evaluated as potent inducers of apoptosis utilizing HTS caspase-based assay [16]. Interestingly, a mammalian protein called secondary mitochondria-derived activator of caspases that triggers apoptosis was identified. This endogenous protein abrogates the inhibitory effects on caspases thus induces caspase-dependent apoptosis [17,18]. Despite these impressive studies, most of the therapeutic applications of this peptide were hampered by its peptide characteristics, such as proteolytic instability. A tetrapeptide motif of the secondary mitochondria-derived activator of caspases was then envisioned as a good lead for designing peptidomimetic compounds as apoptotic inducers in a similar fashion. Towards this approach, a series of capped tripeptides was synthesized to reduce the peptide character of the lead and improve its binding affinity [19]. Pioneering research has led to various small-molecule analogues as efficient apoptotic inducers, and some have shown promising preclinical activity [20,21]. Most recently, optimized fragment-derived nonpeptidomimetic clinical candidates based on amide core were synthesized and evaluated as potential apoptotic inducers [22]. The optimization strategy identified the amide core as an essential part of the molecule that should not be changed.

Taking all together, the current study aims at the design and synthesis of amide-based multifunctional caspase-dependent apoptotic inducers **V** (**Fig. 1**) *via* Passerini reaction. The designed compounds were based on the essential amide core. The substitution pattern was

rationalized to mimic the structural features of lead compounds (**I-IV**) (**Fig. 1**). To gain more information about the structure-activity relationship, various lipophilic and hydrophilic moieties were introduced to the basic scaffold. Towards this goal, our design strategy utilized Passerini multicomponent reaction [23] as a rapid and facial method to generate various substituted amide-based compounds. As our main target compounds, different  $\alpha$ -acyloxy carboxamides were designed and synthesized *via* Passerini reaction utilizing combinations of various aliphatic and aromatic carboxylic acids, cyclohexanone, and *p*-nitrophenyl isocyanide in one-pot reaction protocol. It is worth mentioning that Passerini multicomponent reactions involving *p*-nitrophenyl isocyanide **3** [24] are rare due to the presence of a nitro group (-I, -R), which deactivates the isonitrile nucleophilicity. Herein, we report new efficient optimized conditions to carry out Passerini reactions involving *p*-nitrophenyl isocyanide. Furthermore, investigations of such reactions utilizing different halogenated acids or ninhydrin afforded new unexpected products.

All the newly synthesized target compounds **V** (**Fig. 1**) were screened for cytotoxicity against normal human fibroblasts and their potential anticancer activities against three human cancer cell lines; MCF-7 (breast), NFS-60 (myeloid leukemia), and HepG-2 (liver) utilizing MTT assay [25]. Hence, their respective selectivity indices against the screened cell lines were calculated to assess their efficacy and safety profiles. Compounds exhibiting the most promising anticancer activities were evaluated as caspase-dependent apoptotic inducers utilizing the flow cytometric analysis and caspase 3/7 activation assay. In addition, possible caspase-independent apoptotic pathway through AIF1 was investigated utilizing AIF1 quantification assay. Furthermore, the tested compounds were preliminarily screened for possible antimicrobial activities searching for possible dual anticancer/antimicrobial agents. This desirable dual activity is now viewed as an advantageous approach for cancer therapy [26]. Finally, physicochemical properties, pharmacokinetic profiles, ligand efficiency metrics and drug-likeness data of the tested compounds were computationally predicted as a useful tool for selecting and optimizing lead compounds.

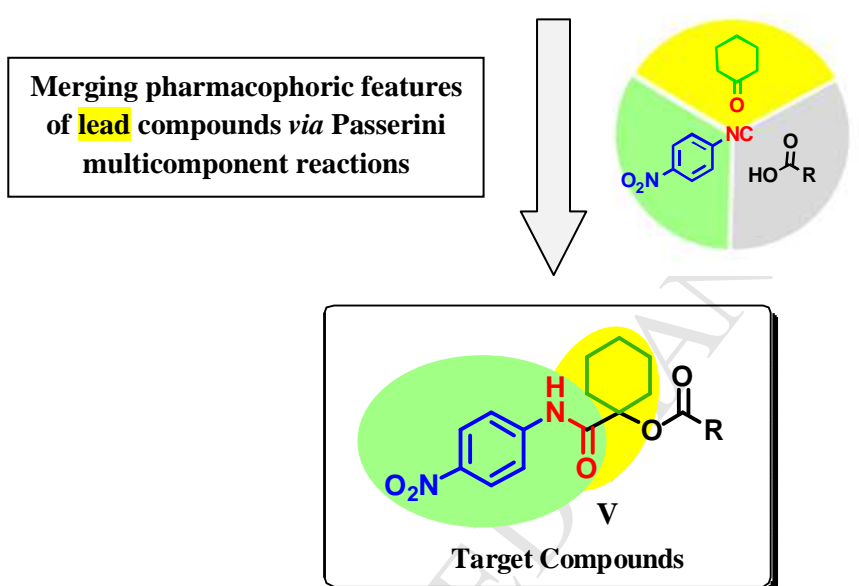
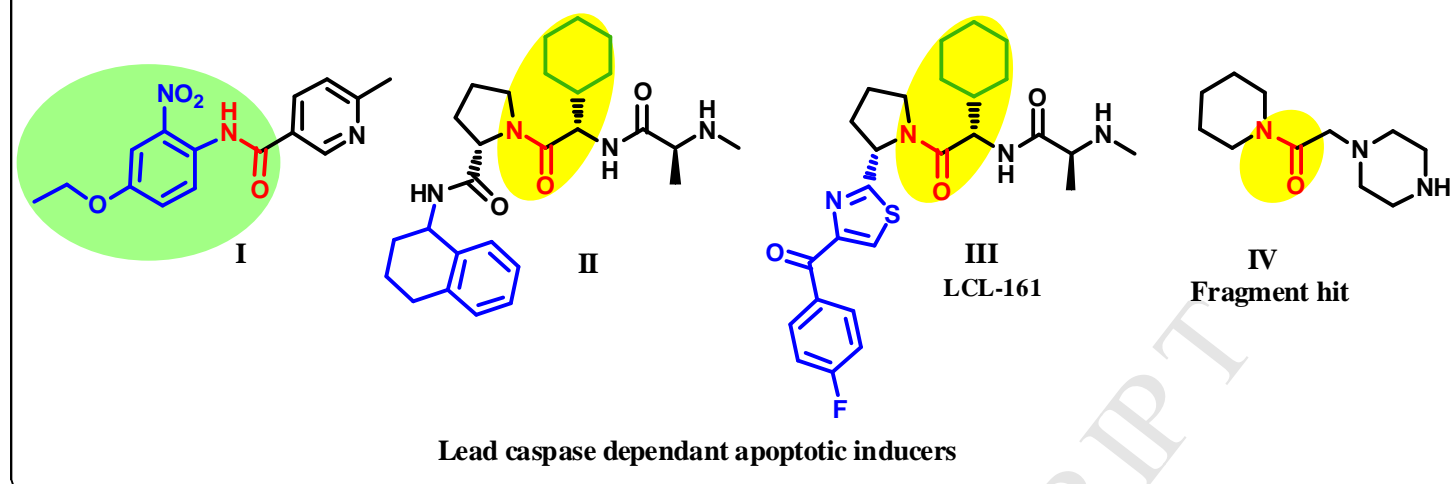
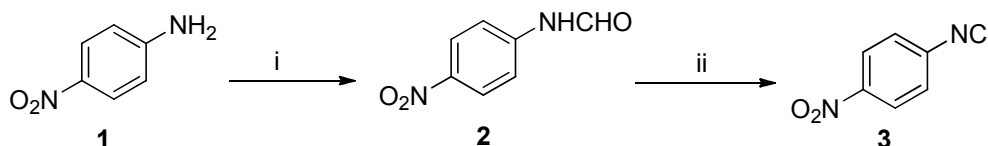


Fig. 1. Rationale for designing the target compounds

## 2. Results and Discussion

### 2.1. Chemistry

Multicomponent reactions are reported as efficient synthetic methods to construct polyfunctional molecules with high diversity and complexity during few steps. Among isocyanide-based multicomponent reactions (IMCR), one-pot combinations of carboxylic acid, ketone and isocyanide were discovered by Passerini in 1921 affording  $\alpha$ -acyloxy carboxamides [23]. Herein, our strategy involved utilizing *p*-nitrophenyl isocyanide **3**, which was synthesized by formylation of *p*-nitroaniline **1** with formic acid in presence of iodine as a catalyst to give *N*-formyl-*p*-nitroaniline **2** [27] followed by dehydration using  $\text{POCl}_3/\text{Et}_3\text{N}$  [28] to afford **3** in good yield (**Scheme 1**). IR of **3** showed the characteristic strong isocyanide band at  $2127\text{ cm}^{-1}$ .



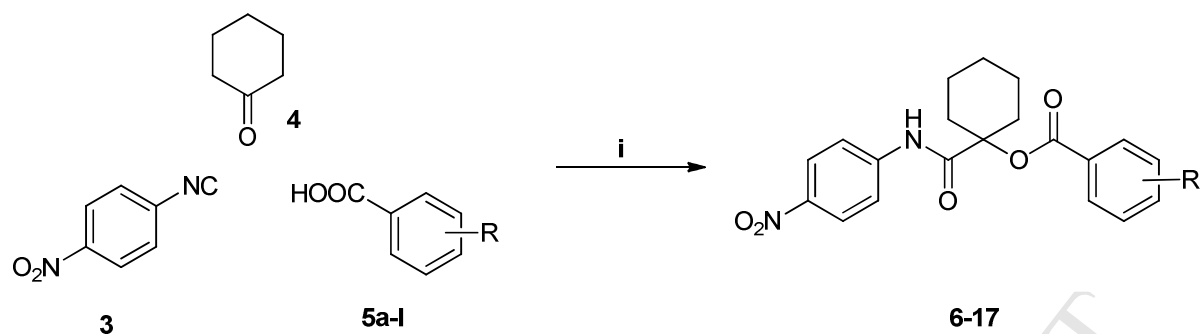
**Reaction conditions:** i. HCOOH, I<sub>2</sub>, Reflux (8 hrs), 86 %;

ii. TEA, DCM/CHCl<sub>3</sub> (2:1), POCl<sub>3</sub>, 0 °C to Reflux (15 min.), 79 %

**Scheme 1.** Synthesis of *p*-nitrophenyl isonitrile **3**

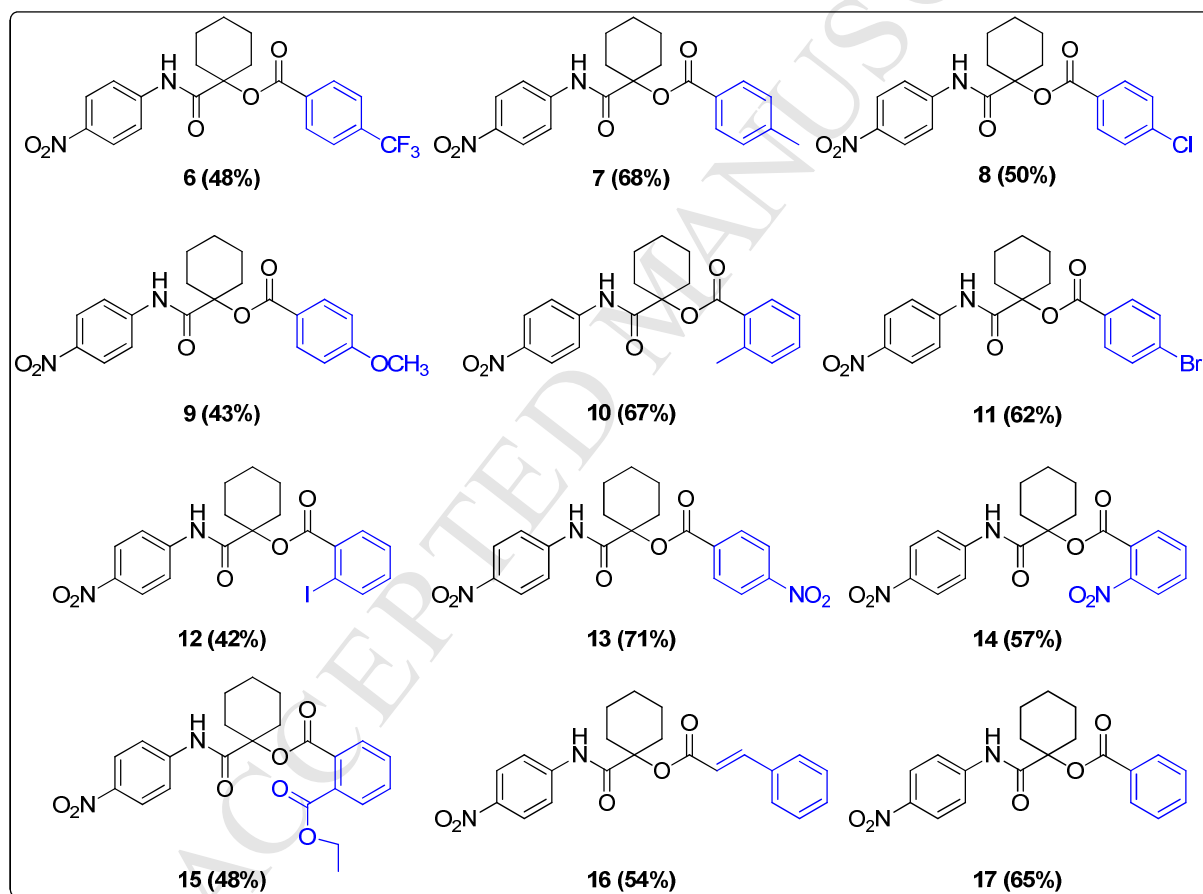
Optimization of Passerini reaction conditions of **3** with cyclohexanone **4** [29] and *o*-nitrobenzoic acid **5i** was accomplished utilizing method A (Reflux in mixture of 2,2,2-trifluoroethanol (TFE) and ethanol co-solvent (1:1)) or method B (stirring in excess cyclohexanone at room temperature) (**supplementary data**). Passerini reaction in other solvents such as DCM, THF, Benzene, Toluene, and *t*-BuOH didn't afford the corresponding  $\alpha$ -acyloxy carboxamide product in the reported time and temperature (**supplementary data**). Regarding method A, the efficiency of TFE/EtOH mixture may be due to combining both, the acidic properties of TFE and the ability to effectively solvate the reaction mixture by EtOH. It is worth mentioning that TFE is a very useful solvent in synthetic chemistry as it possesses an interesting set of properties compared with ethanol; It is more acidic ( $pK_a$  12.5) than ethanol ( $pK_a$  16.0) and has lower nucleophilicity due to the electron-withdrawing effect of the three fluorine atoms [30].

In **Scheme 2**,  $\alpha$ -acyloxy carboxamide derivatives **6-17** were prepared *via* Passerini reaction of **3**, **4** and miscellaneous carboxylic acids **5a-l** incorporating electron withdrawing (-CF<sub>3</sub>, -Cl, -Br, -I, -NO<sub>2</sub>) or electron donating groups (-CH<sub>3</sub>, -OCH<sub>3</sub>) utilizing method A. Passerini reaction utilizing method A didn't afford the expected bis- $\alpha$ -acyloxy carboxamides derivatives in case of phthalic acid **5j** with **3** and **4**. Instead, it afforded ethyl [1-[(4-nitrophenyl)carbamoyl]cyclohexyl] phthalate **15**. This may be attributed to the planarity of phenyl ring preventing the second Passerini reaction due to steric hindrance. The structures of compounds **6-17** were established on the basis of their spectral data. <sup>1</sup>H NMR spectra of **6-17** showed NH signals ( $\delta_H$ : 10.1 - 10.6 ppm) and cyclohexylidene protons ( $\delta_H$ : 1.2-2.6 ppm) at their expected chemical shifts. The characteristic *trans* olefinic protons of the cinnamate derivative **16** appeared at  $\delta_H$ : 7.68 and 6.72 ppm with *J* coupling = 15.5 Hz. <sup>13</sup>C NMR spectra of this series also showed the expected amido-ester C=O groups in the range of  $\delta_C$ : 163.0 to 172.0 ppm. The characteristic cyclohexylidene carbon (O=C-C-O) signals appeared in the range of  $\delta_C$ : 81.0 to 84.5 ppm, while other carbons of the cyclohexyl moiety appeared as three signals ranging from  $\delta_C$ : 20.9 to 32 ppm. <sup>13</sup>C NMR spectrum of **12** showed the characteristic C-I at  $\delta_C$ : 94.7 ppm.



R = a: *p*-CF<sub>3</sub>, b: *p*-CH<sub>3</sub>, c: *p*-Cl, d: *p*-OCH<sub>3</sub>, e: *o*-CH<sub>3</sub>, f: *p*-Br  
 g: *o*-I, h: *p*-NO<sub>2</sub>, i: *o*-NO<sub>2</sub>, j: *o*-COOH, 5k: cinnamic, l: H

Reaction conditions (Method A): i. TFE / EtOH, Reflux (2-12 hrs).

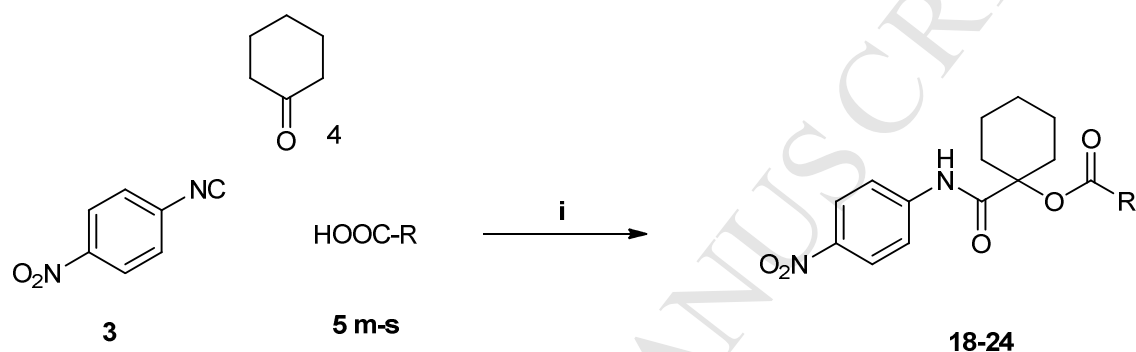


**Scheme 2.** Synthesis of compounds **6-17** via Passerini reaction by method A.

Method A wasn't convenient in case of the utilized aliphatic acids, mandelic acid, phenylacetic acid, and aspirin where all trials led to hydrolysis of **3** to **1**. However, such Passerini reactions carried out by method B [31] were excellent regarding yield and time (**Scheme 3**). The obtained  $\alpha$ -acyloxy carboxamide derivatives **18-24** were confirmed based on spectral data. <sup>1</sup>H NMR spectra of this series showed NH signals ranging from  $\delta_{\text{H}}$ : 10.0 to 10.3 ppm. Protons of cyclohexylidene moiety also appeared in the expected range ( $\delta_{\text{H}}$ : 1.2-2.3 ppm).

$^{13}\text{C}$  NMR spectra showed signals ranging from  $\delta_{\text{C}}$ : 161.0 to 173.0 ppm corresponding to the two amido-ester C=O groups. Cyclohexylidene carbons (O=C-C-O) appeared at the expected range ( $\delta_{\text{C}}$ : 80.0-82.0 ppm). In addition, carbons of the cyclohexyl moiety appeared as three signals ranging from  $\delta_{\text{C}}$ : 20 to 32 ppm.

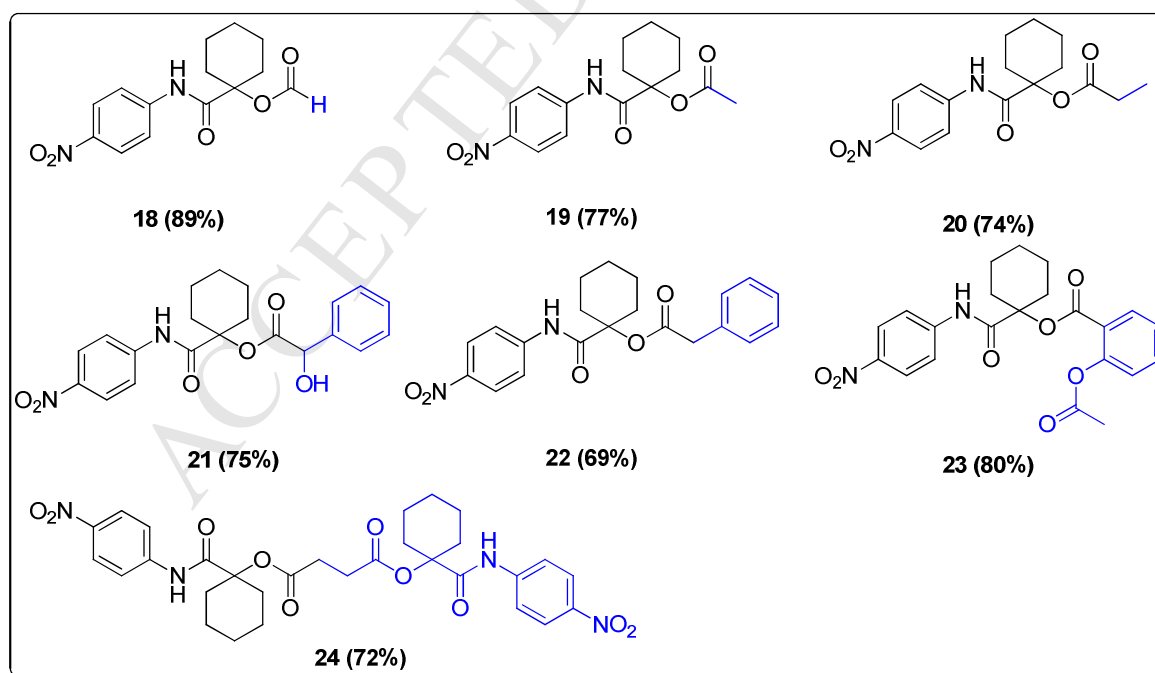
Literature review revealed that synthesis of bis  $\alpha$ -acyloxy carboxamides could be accomplished involving succinic acid [32]. Herein, the target bis  $\alpha$ -acyloxy carboxamide **24** was synthesized by stirring a mixture of succinic acid **5s**, **3**, and **4** utilizing method B. It was proposed that the free rotation of the C-C bond of the two methylene groups may enhance the flexibility to overcome the steric hindrance around the -COOH. EI-MS of **24** showed  $m/z$   $[\text{M}]^+ = 610.47$  (Calcd. = 610.22).



R= m: H, n: CH<sub>3</sub>, o: Et,

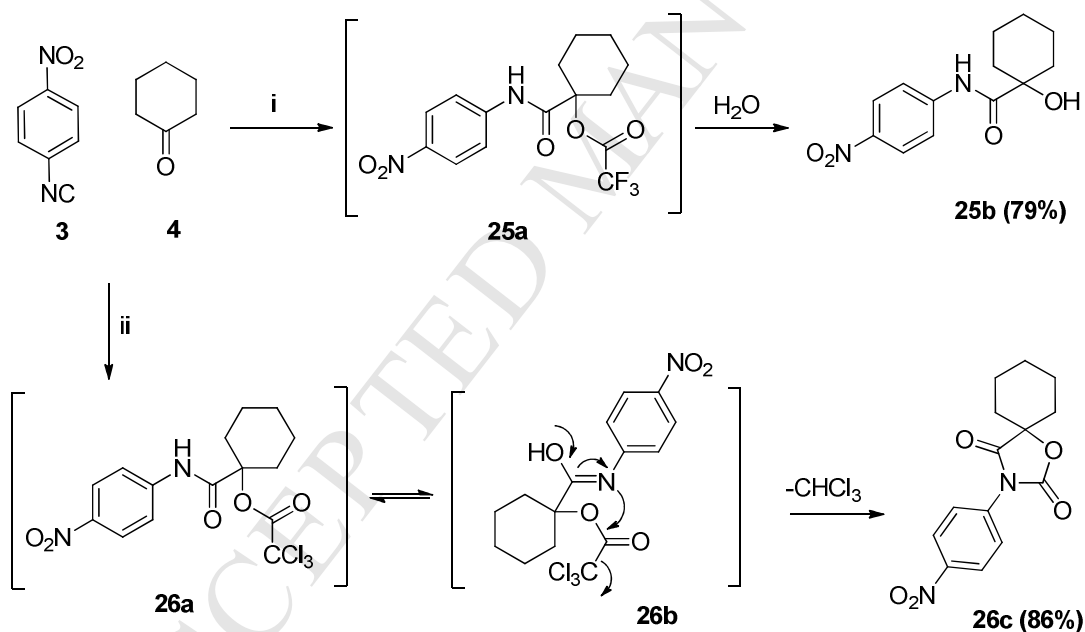
5p: mandelic, 5q: phenylacetic, 5r: aspirin, 5s: succinic acid

Reaction conditions (Method B): i. excess **4**, rt (24 hrs).



**Scheme 3.** Synthesis of compounds **18-24** via Passerini reaction by method B.

Interestingly, Passerini reactions utilizing trihaloacetic acids (**Scheme 4**) gave unexpected products, where trifluoroacetic acid (TFA) afforded 1-hydroxy-*N*-(4-nitrophenyl)cyclohexanecarboxamide **25b** in a good yield. It was proposed that the expected inseparable Passerini product **25a** was completely hydrolyzed [33]. The structure of **25b** was confirmed by  $^1\text{H}$  NMR, where NH and OH protons appeared at  $\delta_{\text{H}}$ : 10.28 and 5.58 ppm, respectively. In addition, its  $^{13}\text{C}$  NMR spectrum showed signals at  $\delta_{\text{C}}$ : 177.1 and 74.0 ppm corresponding to amide carbonyl and tertiary alcohol carbons, respectively. On the other hand, reaction of trichloroacetic acid (TCA) with **4** and **3** proceeded in different manner, where the Passerini product; 1-[(4-nitrophenyl)carbamoyl]cyclohexyl-2,2,2-trichloroacetate **26a** tautomerized to the iminol **26b**. Then internal nucleophilic attack of nitrogen atom on the trichloro acetyl group led to release of the  $-\text{CCl}_3$  and subsequent cyclization to afford the unexpected spiro compound; 3-(4-nitrophenyl)-1-oxa-3-azaspiro[4.5]decane-2,4-dione **26c** [34] (**Scheme 4**). The structure of **26c** was confirmed by  $^1\text{H}$  NMR, where the aromatic protons appeared as two doublets at  $\delta_{\text{H}}$ : 8.39 and 7.81 ppm. In addition, the signals corresponding to the cyclohexylidene protons appeared as expected ( $\delta_{\text{H}}$ : 2.1-1.30 ppm).  $^{13}\text{C}$  NMR showed the characteristic spiro C signal at  $\delta_{\text{C}}$ : 85.1 ppm and the oxazolinedione ring C=O groups [35] at  $\delta_{\text{C}}$ : 173.7 and 152.5 ppm.

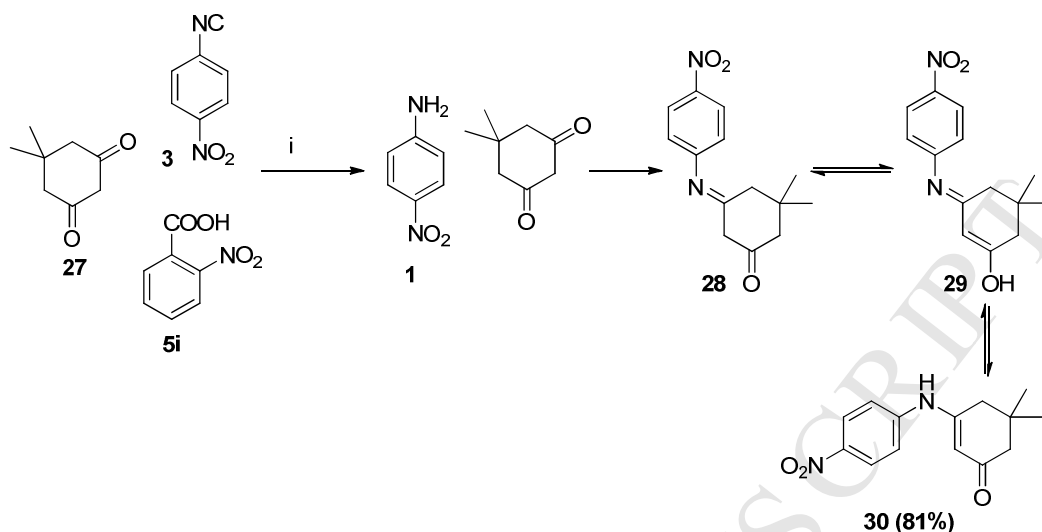


Reaction conditions: i. TFA, rt; ii. TCA, rt (24 hrs).

**Scheme 4.** Synthesis of **26c** and **25b** via Passerini reaction of **3**, **4** and trihaloacetic acids.

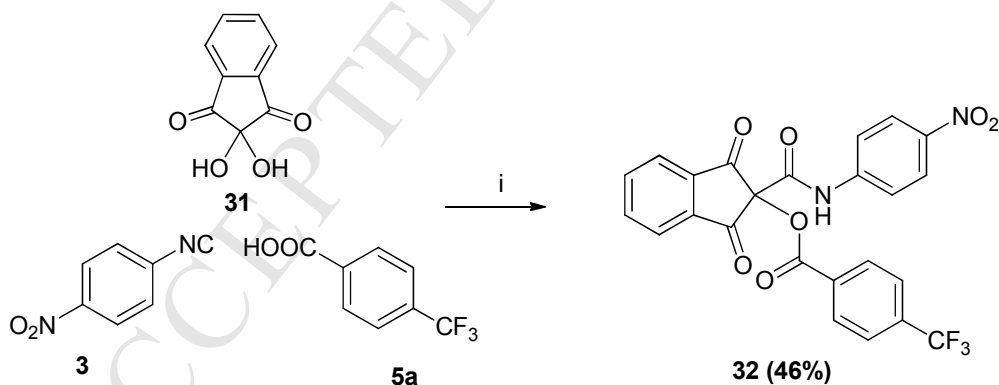
Furthermore, Passerini reaction of **3** with different carbonyl compounds was studied by method A. The reaction of **3** with dimedone **27** and **5i** didn't afford the expected Passerini product. Instead, this reaction led to acidic hydrolysis of **3** to the corresponding amine **1**, which condensed with dimedone to form imine **28** that tautomerized to **29** then to the more stable

isomer  $\alpha$ ,  $\beta$ -unsaturated ketone **30** [36]. Trials utilizing other carboxylic acids also led to the same result (**Scheme 5**).



**Scheme 5.** One-pot reaction of **3** with dimedone and **5i**.

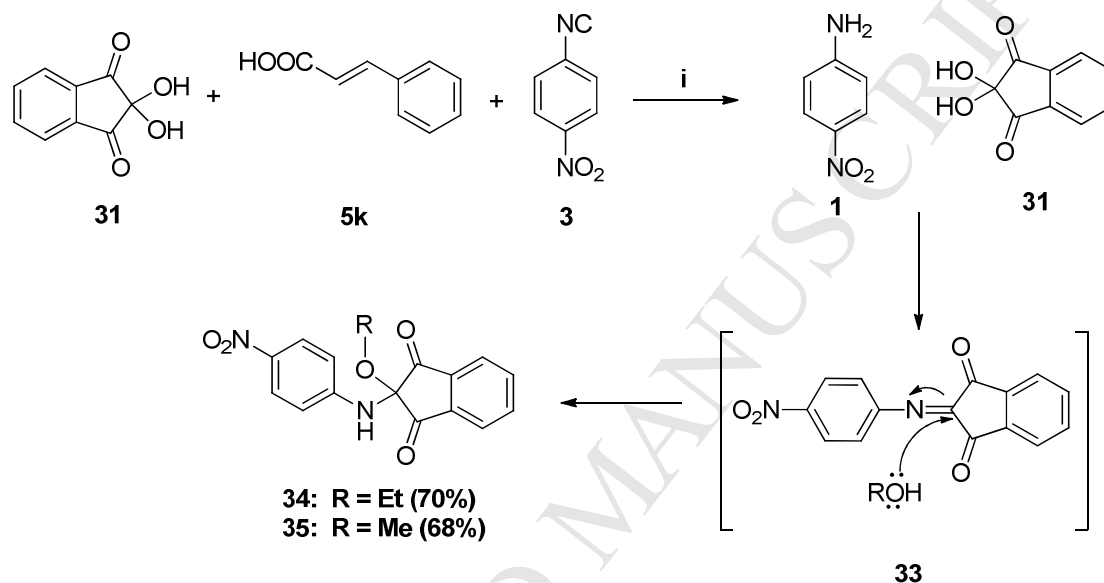
Moreover, Passerini reactions of **3** and ninhydrin **31** utilizing *p*-trifluoromethyl benzoic acid **5a** afforded the expected Passerini product **32** [37] (**Scheme 6**). The structure of **32** was confirmed by  $^1\text{H}$  NMR that showed NH at  $\delta_{\text{H}}$ : 11.42 ppm and aromatic protons at 8.42-7.90 ppm.  $^{13}\text{C}$  NMR spectrum of **32** showed the characteristic indanedione  $\text{sp}^3$  C at  $\delta_{\text{C}}$ : 84.7 ppm as well as the C=O groups at  $\delta_{\text{C}}$ : 190.7 (2C=O), 163.2 (NH-C=O), and 161.5 ppm (O-C=O).



**Scheme 6.** Synthesis of **32** by Passerini reaction of **3** with Ninhydrin **31** and **5a**

On the other hand, boiling a mixture of cinnamic acid **5k**, **3** and ninhydrin in TFE/EtOH (1:1) gave an inseparable mixture of products. Meanwhile, stirring the reaction mixture at room temperature for 16 h led to the unexpected ethyl azaketal **34** in good yield. Replacing EtOH with MeOH afforded the corresponding methyl azaketal **35**. Explanation of this reaction may be illustrated by hydrolysis of **3** to the corresponding amine **1**, which condensed with **31** to

give the imine **33**. The planarity of **33** was proposed to support the addition of EtOH or MeOH to the imine  $\pi$  bond to give the novel azaketals **34** and **35**, respectively in good yields (**Scheme 7**). This proposed mechanism was confirmed by reacting **1** directly with **31** and **5k** in ethanol under the same conditions to afford the same product **34**, which was confirmed by  $^1\text{H}$  NMR showing  $\text{D}_2\text{O}$  exchangeable NH signal at  $\delta_{\text{H}}$ : 8.01 ppm, in addition to the characteristic ethyl protons as quartet ( $\delta_{\text{H}}$ : 3.74 ppm) and triplet ( $\delta_{\text{H}}$ : 1.09 ppm).  $^{13}\text{C}$  NMR spectrum of **34** showed 2  $\text{C}=\text{O}$  and  $\text{NH}-\text{C}-\text{CO}$  at  $\delta_{\text{C}}$ : 193.1 ppm and 82.7 ppm, respectively. Compound **35** was confirmed by  $^1\text{H}$  NMR showing  $\text{D}_2\text{O}$  exchangeable NH signal at  $\delta_{\text{H}}$ : 8.03 ppm, in addition to the methyl protons at  $\delta_{\text{H}}$ : 3.42 ppm.



Reaction conditions: i. TFE/ROH, rt (1 day).

**Scheme 7.** One-pot reaction of **3** with ninhydrin **31** and **5k**.

## 2.2. Biological evaluation

### 2.2.1. Cytotoxicity screening

All the newly synthesized compounds were evaluated for their cytotoxic effects on three human cancer cell lines (MCF-7, NFS-60, HepG-2) and normal human lung fibroblasts (Wi-38) compared to the standard anticancer drug doxorubicin utilizing microculture MTT method [25,38,39] (**Table 1**). Most of the screened compounds showed promising anticancer activities against the tested cell lines, especially MCF-7 (breast cancer). The most potent anticancer activities against MCF-7 cell line were exhibited by compounds **7**, **13**, **21**, **22** and **26c** with single-digit nanomolar  $\text{IC}_{50}$  values. Hence, these compounds were 2-4 folds more active than doxorubicin. Compounds **8**, **14**, **20** and **23** were also more potent than doxorubicin against MCF-7 with  $\text{IC}_{50}$  values in the range of 0.0141-0.0169  $\mu\text{M}$ .  $\text{IC}_{50}$  values of compounds **6** and **35** were comparable to that of doxorubicin, while other screened compounds were less active against MCF-7. Regarding NFS-60 (myeloid leukemia) cell line, compounds **13**, **20**, **21**,

**22** and **26c** were more potent than doxorubicin with single-digit nanomolar  $IC_{50}$  values. In addition, two other compounds (**8** and **23**) showed slightly higher activities ( $IC_{50} = 0.0103$  and  $0.0113 \mu\text{M}$ , respectively) in comparison to the reference. Compounds **6**, **14**, and **34** showed moderate anticancer activities ranging from  $0.0188$  to  $0.0278 \mu\text{M}$ , while the remainders were less active. The antitumor activities of the tested compounds against HepG-2 (liver cancer) revealed two promising compounds (**21** and **26c**) with single-digit nanomolar  $IC_{50}$  values, thus more potent than doxorubicin. In addition, compounds **13** and **22** exhibited comparable anticancer activities to the reference. Other compounds were less active.

Interestingly, results showed that the tested compounds exerted remarkable high safety profiles on normal human lung fibroblasts with  $IC_{50}$  values ranging from  $0.032$  to  $1.964 \mu\text{M}$ , therefore less toxic than doxorubicin ( $IC_{50} = 0.0266 \mu\text{M}$ ). Compounds **25b** and **32** recorded the highest  $IC_{50}$  values ( $1.221$  and  $1.964 \mu\text{M}$ , respectively). Moreover,  $EC_{100}$  (The concentration of the test compound that allows 100% cell viability) values [39] of all the test compounds were higher than doxorubicin, except for compounds **7**, **11**, **14** and **26c**.

While the potency of the screened compounds is an important consideration, assessing their selectivity towards cancer cells is key to the real evaluation of both effectiveness and safety [40]. Such a measure of the drug candidate selectivity towards cancer cells rather than normal cells is known as selectivity index (SI). It is the ratio between the compound  $IC_{50}$  on normal cells and its  $IC_{50}$  on cancer cells. Generally, a drug with  $SI \geq 3$  is considered highly selective [41]. Accordingly, the tested compounds were evaluated based on their selectivity index (SI) values. Herein, all the tested compounds were more selective than doxorubicin against MCF-7 cell lines, except compounds **9**, **10**, **12**, **15**, **16**, **17**, **19** and **30**. Furthermore, compounds **6**, **8**, **13**, **21**, **22**, **23**, **26c** and **32** showed higher selectivity index values than the reference against NFS-60 and HepG-2 cell lines. Interestingly, compounds **8**, **13** and **21** showed the highest selectivity profiles in comparison with other investigated compounds and doxorubicin against all the screened cancer cell lines. Compounds **6**, **22**, **26c** and **32** also showed promising SI values against the three cancer cell lines. Compound **20** showed high SI ( $6.968$ ) against NFS-60 cell line as well as moderate SI ( $3.163$ ) against MCF-7 and lacked selectivity against HepG-2 cells. Moreover, compound **7** was selective against MCF-7 without considerable selectivity against NFS-60 and HepG-2 cells.

**Table 1: *In vitro* cytotoxic activities and selectivity index values (SI) of the tested compounds**

Code	Wi-38		MCF-7		NFS-60		HepG-2	
	IC <sub>50</sub> (μM)*	EC <sub>100</sub> (μM)	IC <sub>50</sub> (μM)	SI	IC <sub>50</sub> (μM)	SI	IC <sub>50</sub> (μM)	SI
6	0.185±0.01	0.0398±0.04	0.0271±0.004	6.826	0.026±0.004	7.115	0.0291±0.001	6.357
7	0.032±0.002	0.0064±0.001	0.0098±0.0003	3.265	0.0454±0.003	0.704	0.0612±0.006	0.522
8	0.355±0.001	0.1128±0.007	0.015±0.005	23.666	0.0103±0.001	34.466	0.0218±0.003	16.284
9	0.04002±0.002	0.0178±0.001	0.0412±0.004	0.970	0.0388±0.003	1.031	0.0571±0.004	0.700
10	0.352±0.006	0.018±0.006	0.516±0.03	0.682	-	-	-	-
11	0.523±0.062	0.0095±0.001	0.237±0.004	2.206	0.236±0.023	2.216	0.284±0.014	1.841
12	0.396±0.01	0.0247±0.016	0.619±0.005	0.639	-	-	-	-
13	0.761±0.048	0.149±0.002	0.0087±0.003	87.471	0.0077±0.002	98.831	0.0141±0.006	53.971
14	0.0346±0.003	0.0067±0.001	0.0147±0.002	2.353	0.0188±0.002	1.840	0.044±0.005	0.786
15	0.386±0.005	0.122±0.011	0.444±0.045	0.869	0.488±0.004	0.790	0.517±0.017	0.746
16	0.041±0.0001	0.0197±0.0001	0.0576±0.003	0.711	0.0505±0.0003	0.811	0.05291±0.001	0.774
17	0.246±0.011	0.148±0.014	0.903±0.01	0.272	0.766±0.081	0.322	0.734±0.047	0.335
18	0.0463±0.001	0.0271±0.001	0.0354±0.001	1.307	0.0338±0.0001	1.369	0.0341±0.002	1.357
19	0.386±0.005	0.122±0.011	0.403±0.008	0.957	0.517±0.01	0.746	0.519±0.008	0.743
20	0.0446±0.006	0.0169±0.002	0.0141±0.003	3.163	0.0064±0.0001	6.968	0.0215±0.002	2.0744
21	0.0844±0.001	0.0507±0.001	0.00501±0.001	16.846	0.0078±0.0016	10.820	0.0077±0.001	10.961
22	0.0439±0.001	0.032±0.0001	0.0077±0.001	5.701	0.0081±0.0008	5.419	0.0142±0.004	3.091
23	0.0484±0.002	0.0355±0.002	0.0169±0.003	2.863	0.0113±0.004	4.283	0.0177±0.003	2.734
24	0.203±0.012	0.020±0.007	-	-	-	-	-	-
25b	1.221±0.0001	0.53±0.002	0.664±0.011	1.838	0.716±0.016	1.705	0.648±0.023	1.884
26c	0.035±0.001	0.006±0.0001	0.0065±0.001	5.384	0.00898±0.0008	3.897	0.0094±0.0001	3.723
30	0.319±0.004	0.157±0.015	0.597±0.013	0.534	0.645±0.006	0.494	0.667±0.003	0.478
32	1.964±0.158	0.635±0.06	0.393±0.015	4.997	0.484±0.043	4.057	0.428±0.004	4.588
34	0.047±0.002	0.0285±0.002	0.0349±0.0004	1.346	0.0278±0.0009	1.690	0.0389±0.004	1.208
35	0.0537±0.001	0.043±0.001	0.0254±0.004	2.114	0.0328±0.003	1.637	0.036±0.004	1.491
DOX	0.0266±0.005	0.0121±0.001	0.0234±0.002	1.136	0.013±0.002	2.046	0.01±0.001	2.66

\*Values are expressed as mean ± SEM

### 2.2.2. Morphological examination of the induced apoptosis

The three cancer cell lines (MCF-7, NFS-60 and HepG-2) were examined for morphological changes when treated with the most active and safe compounds **13**, **21** and **22** in comparison with the untreated cancer cells and cells treated with the reference doxorubicin (**Fig. 2**). As illustrated, all the treated cells obviously lost their normal shapes. Additionally, their characteristic severe shrinkage indicated potent anticancer activities of the tested compounds **13**, **21** and **22** (particularly compound **21**) in comparison to doxorubicin.

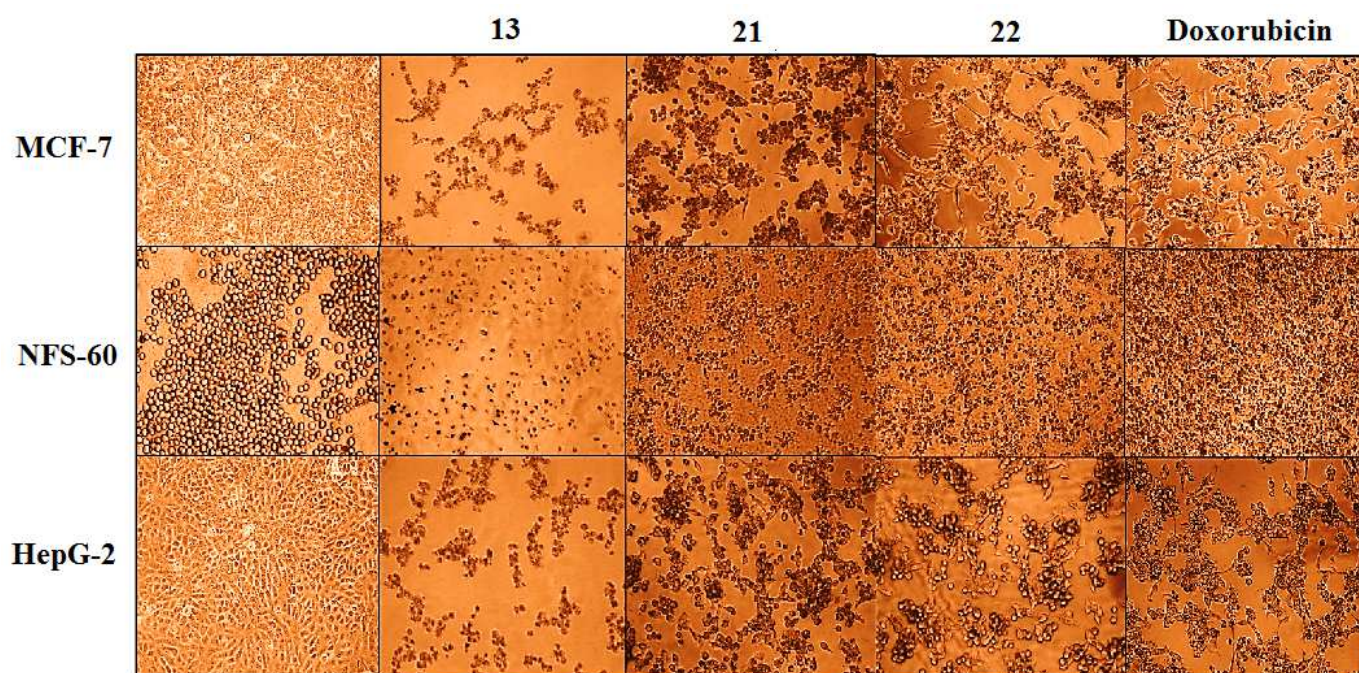


**Fig. 2. Morphological alterations of the most effective compounds-treated cancer cell lines, untreated cancer cells and doxorubicin-treated cells.**

### 2.2.3. Flow cytometric analysis of apoptosis

Compounds **13**, **21** and **22** exhibiting the most promising anticancer activities were tested for their apoptotic effects utilizing flow cytometric annexin V/propidium iodide analysis. In this assay, the cancer cell lines (MCF-7, NFS-60 and HepG-2) were treated with  $IC_{50}$  of the most active compounds for 72 h to study the mode of cell death. The apoptosis-dependent anticancer effects were then determined by quantification of annexin-stained apoptotic cells. Results (**Table 2** and **Fig. 3**) showed high percentages of annexin-stained population cells in cancer cell lines treated with compounds **13**, **21** and **22** compared to the control untreated cancer cells. Compounds **13** and **21** induced apoptosis-dependent death by above 41% in all the treated cancer cell lines compared to less than 37% in case of doxorubicin-treated cells, whereas **22** was comparable to doxorubicin. Interestingly, compound **21** exhibited the highest significant potential for induction of apoptosis (44.185-53.129%), particularly in the late stage of apoptosis (23.6-42.85%) in MCF-7, NFS-60 and HepG-2 cell lines. Compound **13** induced apoptosis by approximately similar percentages (18.43-24.1%) in early and late stages. Meanwhile, no significant difference was observed between the total apoptotic populations (early apoptosis; 6.1-13.6% and late apoptosis; 20.1-27.8%) of **22**- and doxorubicin-treated cancer cells.

**Table 2: Percentages of the apoptotic cell populations in the most effective compounds-treated cancer cells lines.**

Code	MCF-7			NFS-60			HepG-2		
	Early apoptosis %	Late apoptosis %	Total apoptosis %	Early apoptosis %	Late apoptosis %	Total apoptosis %	Early apoptosis %	Late apoptosis %	Total apoptosis %
Negative control	0.47±0.01	0.01±0.001	0.48±0.01 <sup>d</sup>	0.02±0.01	0.015±0.01	0.495±0.01 <sup>d</sup>	0.78±0.09	0.1±0.001	0.169±0.02 <sup>d</sup>
<b>13</b>	24.065±0.96	20.439±2.13	44.505±1.18 <sup>b</sup>	22.83±1.75	18.965±1.41	41.795±0.34 <sup>b</sup>	18.43±1.47	23.385±2.61	41.815±1.14 <sup>b</sup>
<b>21</b>	22.345±1.08	30.785±1.89	53.129±0.81 <sup>a</sup>	21.04±0.7	23.645±0.75	44.185±0.45 <sup>a</sup>	6.055±1.06	42.85±0.97	48.905±0.09 <sup>a</sup>
<b>22</b>	11.885±1.26	22.09±1.52	33.98±0.26 <sup>c</sup>	13.64±1.16	20.09±1.88	34.129±0.42 <sup>c</sup>	6.0649±1.07	27.77±1.19	33.485±0.48 <sup>c</sup>
<b>Dox</b>	13.53±1.35	20.445±1.67	33.974±0.32 <sup>c</sup>	11.379±1.38	23.215±1.6	34.595±0.22 <sup>c</sup>	10.59±1.35	25.49±1.58	36.08±0.23 <sup>c</sup>

\*All values are expressed as mean ± SEM. Different letters are significantly different in the same column at P < 0.05.

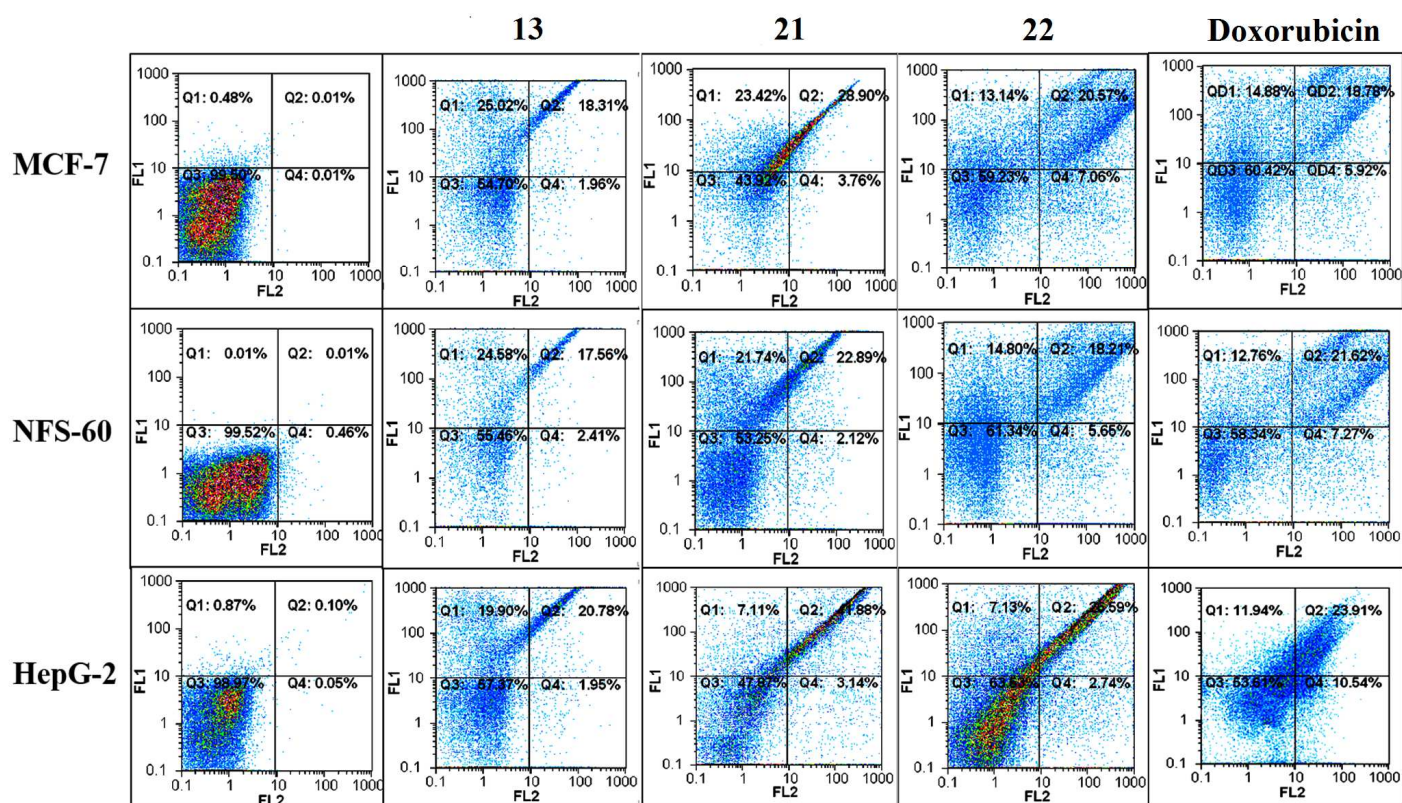


**Fig. 3. Flow charts of annexin-PI analysis of the most effective compounds-treated cancer cells lines, untreated cancer cells and doxorubicin-treated cells.**

#### 2.2.4. Caspase 3/7 activation assay

The mechanism of apoptotic induction exhibited by the most active compounds **13**, **21** and **22** was investigated by determining the percentages of caspase 3/7 activation in cancerous cell lines when treated with IC<sub>50</sub> of these compounds. Results (**Table 3**) revealed that compounds **13** and **21** significantly induced caspase 3/7 activation (more than 49%) higher than the reference; doxorubicin (42.94-48.09%) in all tested human cancer cells. Interestingly,

compound **21** recorded the highest caspase 3/7 activation percentages (52.83-55.04%). Accordingly, results of the caspase 3/7 activation assay were concordant with that of the flow cytometric analysis of apoptosis. Meanwhile, no significant difference was recorded between the percentages of caspase 3/7 activation in compound **22** and doxorubicin-treated cancer cells.

**Table 3: Percentages of caspase 3/7 activation in the most effective compounds-treated cancer cells lines**

Code	Percentage of caspase 3/7 activation		
	MCF-7	NFS-60	HepG-2
<b>13</b>	50.94±0.69 <sup>a</sup>	49.59±0.28 <sup>a</sup>	50.68±0.31 <sup>a</sup>
<b>21</b>	55.04±0.055 <sup>a</sup>	52.835±0.295 <sup>a</sup>	53.64±0.425 <sup>a</sup>
<b>22</b>	43.04±0.29 <sup>b</sup>	45.41±0.59 <sup>b</sup>	47.64±0.77 <sup>b</sup>
<b>Dox</b>	42.94±0.27 <sup>b</sup>	45.39±0.52 <sup>b</sup>	48.09±0.43 <sup>b</sup>

\*All values are expressed as mean ± SEM. Different letters are significantly different in the same column at P < 0.05.

### 2.2.5. Quantification of the apoptosis-inducing factor1 (AIF1)

Based on the fact that cells can undergo caspase-independent apoptosis through AIF1-mediated pathway [12,13], the compounds under investigation (**13**, **21** and **22**) were evaluated utilizing AIF1 quantification assay. Results (**Table 4**) declared that no significant difference in the AIF1 levels was recorded between the untreated cancer cells (MCF-7, NFS-60 and HepG-2 cells) and the most effective anticancer compounds (**13**, **21** and **22**)-treated cell lines. Accordingly, these compounds mediated apoptosis mainly by caspase activation through AIF1-independent pathway.

**Table 4: AIF1 levels (ng/mL) in the most effective compounds-treated cancer cells lines**

	AIF1 (ng/mL)		
	MCF-7	NFS-60	HepG-2
<b>Untreated cells</b>	2.28±0.06 <sup>a</sup>	2.37±0.035 <sup>a</sup>	1.18±0.06 <sup>a</sup>
<b>13</b>	2.34±0.04 <sup>a</sup>	2.44±0.015 <sup>a</sup>	1.28±0.03 <sup>a</sup>
<b>21</b>	2.36±0.015 <sup>a</sup>	2.47±0.01 <sup>a</sup>	1.305±0.01 <sup>a</sup>
<b>22</b>	2.33±0.025 <sup>a</sup>	2.41±0.03 <sup>a</sup>	1.23±0.04 <sup>a</sup>

All values are expressed as mean±SEM. Different letters are significantly different in the same column at P < 0.05.

### 2.3. Antimicrobial evaluation

Selected compounds were evaluated for their *in vitro* antibacterial activities against *Staphylococcus aureus* (ATCC 25923) and *Enterococcus faecalis* (ATCC 29212) as

representatives of Gram-positive bacteria, as well as *Escherichia coli* (ATCC 25922) and *Pseudomonas aeruginosa* (ATCC 27853) as representatives of Gram-negative bacteria. Additionally, their antifungal activities were evaluated against *Candida albicans* (ATCC 90028). The antimicrobial evaluation protocol is rationalized to screen the tested compounds for possible antimicrobial activities utilizing the agar well diffusion assay [42] (**supplementary data**). The compounds showing antimicrobial activities were then evaluated for their minimum inhibitory concentrations through the standard broth microdilution method [43] (**Table 5**).

All the screened compounds showed detectable inhibition zones except **6**, **7** and **16**. Accordingly, minimum inhibitory concentrations of the selected compounds were measured against their respective sensitive microorganisms. Generally, all the tested compounds showed weak antimicrobial activities relative to the standards. Compound **34** showed antibacterial activity only against *S. aureus* with MIC = 1.569  $\mu\text{M}/\text{mL}$ , while compounds **8**, **9**, **14**, **18**, **21**, **22**, **23**, **26c** and **35** were slightly active against *E. coli* with compound **8** showing the lowest MIC (1.271  $\mu\text{M}/\text{mL}$ ) among the group. All compounds showed no detectable antifungal activity except for compound **25** which exhibited weak activity against *C. albicans* with MIC = 1.040  $\mu\text{M}/\text{mL}$ .

**Table 5: Antimicrobial evaluation of the tested compounds by microdilution assay.**

Code	MIC ( $\mu\text{M}/\text{mL}$ )		
	<i>S. aureus</i>	<i>E. coli.</i>	<i>C. albicans</i>
<b>8</b>	NA*	1.271	NA
<b>9</b>	NA	2.570	NA
<b>14</b>	NA	2.477	NA
<b>18</b>	NA	3.503	NA
<b>21</b>	NA	2.570	NA
<b>22</b>	NA	2.677	NA
<b>23</b>	NA	2.401	NA
<b>25</b>	NA	NA	1.040
<b>26c</b>	NA	3.527	NA
<b>34</b>	1.569	NA	NA
<b>35</b>	NA	3.279	NA
<b>Ciprofloxacin</b>	0.006	0.003	-
<b>Fluconazole</b>	-	-	0.001

\*NA: No activity

#### **2.4. In silico prediction of physicochemical properties, drug-likeness data and ligand efficiency metrics**

The drug discovery sector now utilizes the computational prediction of physicochemical properties and drug-likeness data as a useful tool to identify drug candidates. In the current study, we applied various computational methods to assess whether the most active compounds possess the optimum drug-likeness parameters or not. *Molinspiration* [44]

software was employed to predict the descriptors formulating Lipinski's rule of five [45], which states that oral bioavailability and cell permeability are possible if at least three rules of the following five are obeyed: *n*-octanol-water partition coefficient ( $\log P$ )  $\leq 5$ , molecular weight (M.Wt)  $\leq 500$  Da, number of hydrogen bond donors (HBD)  $\leq 5$  and number of hydrogen bond acceptors (HBA)  $\leq 10$ . Accordingly, Lipinski's violation could be predicted. *Molinspiration* also calculated the number of rotatable bonds (NROTb) and topological polar surface area (TPSA) as useful descriptors of oral bioavailability of drug candidates [46]. As estimated, TPSA values for most known drugs are below 140–150 Å<sup>2</sup> [47,48]. The percentage of absorption could be also predicted based on TPSA applying the following equation: %ABS=109–0.345TPSA. Accordingly, *in silico* physicochemical properties of all the synthesized compounds were calculated (Table 6).

**Table 6: *In silico* physicochemical properties of the tested compounds as predicted by *Molinspiration***

Code	LogP <sup>a</sup>	M.Wt <sup>b</sup>	HBA <sup>c</sup>	HBD <sup>d</sup>	Lipinski's Violation	TPSA <sup>e</sup>	%ABS <sup>f</sup>	Volumes (Å) <sup>3</sup>	NROTb <sup>g</sup>
6	5.74	436.39	7	1	1	101.23	74.07	359.11	7
7	5.29	382.42	7	1	1	101.23	74.07	344.37	6
8	5.52	402.83	7	1	1	101.23	74.07	341.35	6
9	4.90	398.42	8	1	0	110.46	70.89	353.36	7
10	4.91	382.42	7	1	0	101.23	74.07	344.37	6
11	5.66	447.29	7	1	1	101.23	74.07	345.70	6
12	5.54	494.29	7	1	1	101.23	74.07	351.80	6
13	4.80	413.39	10	1	0	147.05	58.26	351.14	7
14	4.94	413.39	10	1	0	147.05	58.26	351.14	7
15	4.67	440.45	9	1	0	127.53	65.00	389.14	9
16	5.26	394.43	7	1	1	101.23	74.07	355.23	7
17	4.85	368.39	7	1	0	101.23	74.07	327.81	6
18	2.84	292.29	7	1	0	101.23	74.07	256.40	5
19	3.12	306.32	7	1	0	101.23	74.07	272.96	5
20	3.48	320.35	7	1	0	101.23	74.07	289.76	6
21	3.73	398.42	8	2	0	121.45	67.09	352.66	7
22	4.72	382.42	7	1	0	101.23	74.07	344.61	7
23	4.43	426.43	9	1	0	127.53	65.00	372.34	8
24	5.44	610.62	14	2	3	202.45	39.15	533.77	13
25b	2.42	264.28	6	2	0	95.15	76.17	236.45	3
26c	3.01	290.27	7	0	0	92.44	77.10	245.94	2
30	3.11	260.29	5	1	0	74.92	83.15	238.57	3
32	4.31	498.37	9	1	0	135.37	62.29	384.48	7
34	2.64	326.31	7	1	0	101.23	74.07	277.17	5
35	2.27	312.28	7	1	0	101.23	74.07	260.36	4

<sup>a</sup>Log P: logarithm of compound partition coefficient between *n*-octanol and water.

<sup>b</sup>M.Wt: molecular weight.

<sup>c</sup>HBA: number of hydrogen bond acceptors.

<sup>d</sup>HBD: number of hydrogen bond donors.

<sup>e</sup>TPSA: polar surface area.

<sup>f</sup>%ABS: percentage of absorption.

<sup>g</sup>NROTb: number of rotatable bonds.

Most of the screened compounds were in full accordance to Lipinski's rule of five. Compounds **6, 7, 8, 11, 12** and **16** showed slight violation regarding log P, while compound **24** didn't obey Lipinski's rule regarding log P, M.Wt and HBA. TPSA values of all compounds were in the acceptable range except for **24**. Hence, most of the tested compounds displayed reasonable %ABS in the range of 58.26–83.15% indicating promising predicted oral bioavailability. *Molsoft* software [49] was employed to predict solubility and drug-likeness model scores of the tested compounds (**Table 7**). About 80% of marketed drugs have an estimated solubility above 0.0001 mg/L. Interestingly; all tested compounds fulfill this solubility requirement, except **24** and **32**. Compounds **18, 19, 20, 25b** and **26c** recorded remarkable predicted solubility profiles. Finally, the drug-likeness model score; a collective descriptor of the predicted physicochemical properties, pharmacokinetics and pharmacodynamics parameters, was predicted for each compound [50]. Compounds with zero or negative values should not be considered as drug-like. As illustrated (**Table 7**), compounds **10, 12, 15, 21** and **23** recorded positive drug-likeness values indicating good predicted drug-likeness potential. Taking all together, it could be concluded that the most active compounds exhibited reasonable physicochemical properties and drug-likeness values, which might raise them to be drug-like candidates.

**Table 7: *In silico* drug-likeness data of the tested compounds as predicted by *Molsoft***

Code	S <sup>a</sup> (mg/L)	Drug-likeness model score
<b>6</b>	0.04	-0.63
<b>7</b>	0.19	-0.43
<b>8</b>	0.06	-0.08
<b>9</b>	0.32	-0.35
<b>10</b>	0.24	0.05
<b>11</b>	0.28	-0.41
<b>12</b>	0.08	0.18
<b>13</b>	0.08	-0.48
<b>14</b>	0.31	-0.35
<b>15</b>	1.76	0.17
<b>16</b>	0.09	-0.68
<b>17</b>	0.53	-0.59
<b>18</b>	71.66	-0.63
<b>19</b>	25.54	-0.63
<b>20</b>	14.19	-0.32
<b>21</b>	1.31	0.25
<b>22</b>	1.33	-0.53
<b>23</b>	0.61	0.60
<b>24</b>	0.00	-0.46
<b>25b</b>	25.83	-0.47
<b>26c</b>	25.33	-0.57
<b>30</b>	3.22	-1.13
<b>32</b>	0.00	-0.65
<b>34</b>	1.42	-0.87
<b>35</b>	2.36	-1.07

S<sup>a</sup> aqueous solubility

Recently, medicinal chemists utilize ligand efficiency (LE) as a useful parameter for selecting and optimizing lead compounds. This metric represents the balance of potency and molecular size, which is related to many pharmacokinetic and toxicological parameters [51–53]. It measures the average binding energy contribution per non-hydrogen atom instead of considering the binding affinity or potency of the whole molecule. Accordingly, this approach allows comparing and prioritizing the screened ligands corrected for their sizes [54].

LE can be calculated from following equations [54].

$$LE = \Delta G / NHA = 1.37 (\text{pIC}_{50}) / NHA$$

Where:

$\Delta G$  = Gibb's free energy

NHA = non-hydrogen atom.

$\text{pIC}_{50}$  = half-maximal inhibitory concentration (in term of molar concentration).

The lower acceptable limit of LE is 0.3 [55].

The concept of ligand efficiency has been extended to consider other important physicochemical properties, such as lipophilicity. This allows the introduction of the new metric Lipophilic Ligand Efficiency (LLE). LLE is defined as a measure of how efficiently a ligand exploits its lipophilicity to bind to a given target [56]. Monitoring LLE can thus highlight the price paid in lipophilicity on the expense of potency. This parameter can be calculated as the difference between log P and the negative logarithm of a potency measure ( $\text{pIC}_{50}$ )

$$LLE = \text{pIC}_{50} - \text{cLog P}$$

LLE values  $\geq 3$  are considered acceptable for lead compounds, while values  $\geq 5$  are recommended for drug-like candidates [55,57]

In the current study, LE and LLE values of all the synthesized compounds were calculated based on their respective  $\text{IC}_{50}$  values against the screened cancer cell lines utilizing the previously mentioned equations. Results (**Table 8**) indicated that all the tested compounds had acceptable LE values ( $> 0.3$ ) against MCF-7, NFS-60, and HepG-2 cell lines except **15**, **24** and **32**. Compound **26c** showed the highest LE values against MCF-7 and HEpG-2 cells (0.534 and 0.523, respectively), while compound **20** showed the highest LE value against NFS-60 (0.547). Concerning LLE, compounds **26c** and **35** showed the highest drug-like LLE values ( $>5$ ) against the three screened cancer cell lines. Moreover, compound **20** showed remarkable LLE (5.713) against NFS-60 cell lines and lead like value against other cell lines. Compounds **13**, **18**, **19**, **21**, **22**, **23**, **25b**, **30** and **34** exhibited LLE values above the recommended limit for lead compounds ( $>3$ ) against all the screened cancer cells. Other compounds were beyond the acceptable limit (0.668-2.892).

**Table 8: Ligand Efficiency (LE) and Ligand Lipophilic Efficiency (LLE) of the tested compounds.**

Code	NHA <sup>a</sup>	LogP <sup>b</sup>	MCF-7			NFS-60			HepG-2		
			pIC <sub>50</sub> <sup>c</sup>	LE	LLE	pIC <sub>50</sub>	LE	LLE	pIC <sub>50</sub>	LE	LLE
6	31	5.74	7.567	0.334	1.827	7.585	0.335	1.845	7.536	0.333	1.79
7	28	5.29	8.008	0.391	2.718	7.342	0.359	2.052	7.213	0.352	1.923
8	28	5.52	7.823	0.382	2.303	7.987	0.390	2.467	7.661	0.374	2.141
9	29	4.90	7.385	0.348	2.485	7.411	0.350	2.511	7.243	0.342	2.343
10	28	4.91	6.287	0.307	1.377	-	-	-	-	-	-
11	28	5.66	6.625	0.324	0.965	6.627	0.324	0.967	6.546	0.320	0.886
12	28	5.54	6.208	0.303	0.668	-	-	-	-	-	-
13	30	4.80	8.060	0.368	3.26	8.113	0.370	3.313	7.850	0.358	3.05
14	30	4.94	7.832	0.357	2.892	7.725	0.352	2.785	7.356	0.335	2.866
15	32	4.67	6.352	0.271	1.68	6.311	0.270	1.641	6.286	0.269	1.616
16	29	5.26	7.239	0.341	1.979	7.296	0.344	2.036	7.276	0.343	2.016
17	27	4.85	6.044	0.306	1.194	6.115	0.310	1.265	6.134	0.311	1.284
18	21	2.84	7.450	0.486	4.610	7.471	0.487	4.631	7.467	0.487	4.627
19	22	3.12	6.394	0.398	3.274	6.286	0.391	3.166	6.284	0.391	3.164
20	23	3.48	7.850	0.467	4.370	9.193	0.547	5.713	7.667	0.456	4.187
21	29	3.73	8.300	0.392	4.570	8.107	0.382	4.377	8.113	0.383	4.383
22	28	4.72	8.113	0.396	3.393	8.091	0.395	3.371	7.847	0.383	3.127
23	31	4.43	7.772	0.313	3.342	7.946	0.351	3.516	7.752	0.342	3.322
24	44	5.44	-	-	-	-	-	-	-	-	-
25b	19	2.42	6.177	0.445	3.757	6.145	0.443	3.725	6.188	0.446	3.768
26c	21	3.01	8.187	0.534	5.177	8.046	0.524	5.036	8.026	0.523	5.016
30	19	3.11	6.224	0.448	3.114	6.190	0.446	3.080	6.175	0.445	3.065
32	36	4.31	6.405	0.243	2.095	6.315	0.240	2.005	6.368	0.242	2.058
34	24	2.64	7.457	0.425	4.817	7.555	0.431	4.915	7.410	0.422	4.77
35	23	2.27	7.595	0.452	5.325	7.484	0.445	5.214	7.443	0.443	5.173

<sup>a</sup>LogP: logarithm of compound partition coefficient between n-octanol and water.

<sup>b</sup>NHA = non-hydrogen atom.

<sup>c</sup>pIC<sub>50</sub> = -log (IC<sub>50</sub>)

### 3. Structure activity relationship

The general activity pattern suggests that the designed amide-based scaffold conserved the intrinsic anticancer effect of the reported lead apoptotic inducers (**Fig. 1**). However, activity and selectivity were found to be a function of the substitution nature and size.

Seemingly, most of the target amide esters showed relatively better anticancer activities than the unexpected azaketals **34** and **35**, hydroxy derivative **25b** and  $\alpha$ ,  $\beta$ -unsaturated ketone **30**. However, the unexpected spiro compound **26c** was among the most active compounds against the three screened cell lines with single-digit nanomolar IC<sub>50</sub> values.

Within the evaluated esters, the mandelate ester **21** conferred the highest activities against MCF-7 and HepG-2 cells. In addition, it showed promising activity against NFS-60 cell

lines. The absence of the  $\alpha$ -hydroxy group led to slightly less active derivative **22**. It is worth mentioning that both **21** and **22** were more potent than the reference against MCF-7 and NFS-60 cells. Moreover,  $\alpha$ -vinylic moiety of the cinnamate ester **16** dramatically decreased the anticancer activities against the three cell lines. Obviously, benzoate esters showed variable anticancer activities according to the aromatic ring substitution pattern. In this series, the *p*-nitro derivative **13** was among the three most active compounds of the current study. Shifting the nitro group to *ortho*- position (**14**) slightly decreased the antitumor activities against the screened cell lines. On the other hand, *p*-methyl group (**7**) conferred high potency against MCF-7 cells, moderate activity against NFS-60 and weak activity against HepG-2 cells. Oxygen insertion (*p*-methoxy derivative **9**) critically decreased the anticancer activity against MCF-7 cells, while allowing a slight increase in activity regarding NFS-60 and HepG-2 cells. Shifting the methyl group to *ortho*- position (**10**) also decreased the anticancer activity against MCF-7 cells, but abolished activity against both NFS-60 and HepG-2 cell lines. Interestingly, replacing *p*-methyl group (**7**) with *p*-trifluoromethyl (**6**) endowed remarkable potency against the three cancer cell lines, especially NFS-60 and HepG-2 cell lines. Concerning halogenated derivatives, the *p*-chloro derivative **8** displayed promising activities against MCF-7 and NFS-60 cells (higher than the reference) and moderate effect against HepG-2, while the *p*-bromo derivative **11** was 10-20 folds less active against the three cell lines. Furthermore, the *o*-iodo derivative **12** was the least active among the group with no considerable activity against NFS-60 and HepG-2 cell lines. Results also showed that derivatives with *o*-esters (**15** and **23**) were active against the screened cell lines. However, the methyl ester (**23**) conferred much more potency to the molecule than the ethyl ester (**15**) did. In comparison to the previously mentioned compounds, the unsubstituted benzoate derivative **17** was less active towards the screened cell lines. Furthermore, replacing the aromatic ring with aliphatic moieties also controlled both activity and selectivity. Among this series, the propionate ester **20** showed higher potency than the standard drug against both MCF-7 and NFS-60, as well as acceptable activity against HepG-2 cells. The formate ester **18** was slightly less active than **20** against the three cell lines with no detected selectivity, while the acetate ester **19** was the least active. Obviously, the bis  $\alpha$ -acyloxy carboxamide derivative **24** was inactive against the screened cell lines. Also, the indenyl benzoate derivative **32** showed much lower activity the corresponding cyclohexyl derivative **6**.

#### 4. Conclusion

This study portrays the design and synthesis of new multifunctional Passerini compounds. *In vitro* cytotoxicity screening against three cancerous and one normal human cell lines revealed that most of these compounds showed promising anticancer activities against all the screened cancer cell lines with acceptable safety and selectivity profiles. Among tested compounds, **7**, **8**, **13**, **14**, **20**, **21**, **22**, **23** and **26c** were more potent than doxorubicin against MCF7 cell line, while IC<sub>50</sub> values of compounds **6** and **35** were comparable to that of the reference. Regarding NFS-60 cell line, compounds **8**, **13**, **20**, **21**, **22**, **23** and **26c** showed higher IC<sub>50</sub> values in comparison to doxorubicin. Furthermore, compounds **13**, **21**, **22**, **23** and **26c** exhibited higher or comparable anticancer activity to the reference against HepG-2 cancer cell line. The tested compounds were also evaluated for their safety based on their selectivity index

(SI) values. Compounds **6**, **8**, **13**, **21**, **22**, **26c** and **32** were the safest ones, showing the highest selectivity profiles in comparison with other investigated compounds and doxorubicin against NFS-60, MCF-7 and HepG-2 cell lines. Compounds **13**, **21** and **22** were selected for further mechanistic studies. The three compounds significantly induced apoptosis by caspase activation in all the screened cancer cell lines utilizing flow cytometric analysis and caspase 3/7 activation assay. Both **13** and **21** were more potent caspase 3/7 activators than doxorubicin, while **22** showed comparable results. Furthermore, evaluation utilizing quantification of AIF1 assay excluded possible AIF1-mediated apoptotic induction and clarified that **13**, **21** and **22** were caspase-dependent apoptotic inducers. Physicochemical parameters, ligand efficiency metrics and drug-likeness data of the all the evaluated compounds were computationally predicted. *In silico* results showed that compounds **13**, **21** and **22** may be considered as drug-like candidates. Finally, selected compounds were preliminarily screened for possible antimicrobial activities searching for possible dual anticancer/ antimicrobial agents as an advantageous approach for cancer therapy. Although, results revealed weak antimicrobial activities, compounds **21** and **22** were slightly active against *E. coli*. Therefore, it could be concluded that Passerini based amides may hold promise for a new scaffold of caspase activators that deserve further studies. Compounds **13**, **21** and **22** may be considered as selective anticancer leads inducing apoptosis *via* caspase activation mechanism with promising predicted drug likeness data.

## 5. Experimental

### 5.1. Chemistry

#### 5.1.1. General experimental information

All reactions were carried out in dried glassware. Triethylamine and Trifluoroethanol were purchased and used without further purification. NMR spectra were measured using a JEOLJNM ECA 500 or 400 MHz. The deuterated solvent was used as an internal deuterium lock.  $^{13}\text{C}$  NMR spectra were recorded using the UDEFT pulse sequence and broad band proton decoupling at either 100 or 125 MHz. All chemical shifts ( $\delta$ ) are stated in units of parts per million (ppm) and presented using TMS as the standard reference point. Melting points were recorded using Thermo Scientific, Model NO: 1002D, 220-240v; 200watts; 50/60Hz and are uncorrected. Mass spectra were carried out on direct probe controller inlet part to single quadropole mass analyzer in (Thermo Scientific EIMS), Model: ISQ LT, using thermo x-calibur software. Values are reported as a ratio of mass to charge ( $m/z$ ) in Daltons. IR [ $\text{v}/\text{cm}^{-1}$ ] data were recorded using Perkin Elmer; FT-IR Spectrum BX and Bruker tensor 37 FT-IR. Visualization of the TLC during monitoring of the reaction was done by UV VILBER LOURMAT 4w-365nm or 254nm tube.

#### Synthesis of *p*-nitrophenyl formamide (**2**)

Iodine (0.46 g, 0.003 mol) was added to a solution of *p*-nitroaniline **1** (10 g, 0.07 mol) in formic acid (50 ml). The mixture was stirred under Reflux for 8 hours. After completion of the reaction, the reaction was kept overnight at room temperature. The precipitate of the desired

product was collected by filtration, washed by a solution of  $\text{Na}_2\text{S}_2\text{O}_3$ , and water to give **2** [27], a pale yellow crystals, (10 gm, 86%) Mp= 196-199 °C, [lit.[58] Mp =197.5-198 °C]

### Synthesis of *p*-nitrophenyl isocyanide (**3**)

In a three neck round-bottomed flask compound **2** (10 g, 0.06 mol) was added to solution of  $\text{Et}_3\text{N}$  (41.9 mL, 0.3 mol) in a mixture of  $\text{CHCl}_3/\text{DCM}$  (1:2, 50 mL). The mixture was stirred in an ice bath for 10 minutes.  $\text{POCl}_3$  (6.1 ml, 0.066 mol) was added to the stirred mixture [28] till the color of mixture turned to the dark brown. Then the mixture was stirred under Reflux for 15 minutes. The reaction was quenched by adding cold water (50 mL), then, the mixture was washed with  $\text{CHCl}_3$  (3 × 50 mL). The organic layers were combined, dried over anhydrous sodium sulfate, filtered and evaporated under reduced pressure to afford **3** (7.2 gm, 79 %) as orange solid; Mp=116-118 °C; [lit.[59] MP =119-120 °C]; IR:  $\nu_{\text{max}}/\text{cm}^{-1}$  2127 (-NC), 1572 ( $\text{NO}_2$ ), 1346 ( $\text{NO}_2$ );  $^1\text{H NMR}$  (500 MHz,  $\text{DMSO-}d_6$ )  $\delta_{\text{H}}$ : 7.92 (d,  $J = 9$  Hz, 2H), 7.55 (d,  $J = 9$  Hz, 2H).

#### 5.1.2. General method A for Passerini reactions

*p*-Nitrophenyl isocyanide **3** (50 mg, 0.337 mmol, 1.1 eq) was added to a solution of cyclohexanone (0.337 mmol, 1.1 eq), and the appropriate carboxylic acid (0.307 mmol, 1.0 eq) in a mixture of 2,2,2-trifluoroethanol (TFE) and ethanol (1:1, 2 mL). The mixture was stirred under Reflux. The reaction was monitored by TLC. After the reaction completion, the mixture was cooled to precipitate the desired product. The product was filtered, washed with a saturated solution of  $\text{NaHCO}_3$ , dried and collected without further purification.

#### 1-[(4-Nitrophenyl)carbamoyl]cyclohexyl-4-(trifluoromethyl)benzoate (**6**)

Yield 48%; off white powder; Mp= 232-237°C;  $R_f$  0.76 (EtOAc - petroleum ether, 1:2); IR:  $\nu_{\text{max}}/\text{cm}^{-1}$  3297 (NH), 1729 (CO), 1681 (OCN);  $^1\text{H NMR}$  (500 MHz,  $\text{DMSO-}d_6$ )  $\delta_{\text{H}}$ : 10.22 (s, 1H, NH), 8.21 (d,  $J = 8.4$  Hz, 2H, Ar-H), 8.16 (d,  $J = 9.1$  Hz, 2H, Ar-H), 7.92 (d,  $J = 7.6$  Hz, 2H, Ar-H), 7.85 (d,  $J = 9.1$  Hz, 2H, Ar-H), 2.29 (d,  $J = 13.7$  Hz, 2H, Cyclohex-H), 1.90 (dist.t,  $J = 12.2, 11.4$  Hz, 2H, Cyclohex-H), 1.66 (bs, 3H, Cyclohex-H), 1.60 - 1.52 (m, 2H, Cyclohex-H), 1.35 - 1.28 (m, 1H, Cyclohex-H);  $^{13}\text{C NMR}$  (125 MHz,  $\text{DMSO-}d_6$ )  $\delta_{\text{C}}$ : 171.8 (NH-C=O), 163.9 (O-C=O), 145.6, 142.9, 134.0, 131.0, 130.9, 126.3, 125.2, (Ar-C), 125.1 ( $\text{CF}_3$ ), 120.3 (Ar-C), 82.9 (O=C-C-O), 31.8, 25.0, 21.6 (Cyclohex-C); EI-MS,  $m/z$  [M]<sup>+</sup> calcd for  $[\text{C}_{21}\text{H}_{19}\text{F}_3\text{N}_2\text{O}_5]^+$ : 436.12, found 436.52; Anal. calcd. for  $\text{C}_{21}\text{H}_{19}\text{F}_3\text{N}_2\text{O}_5$ : C, 57.80; H, 4.39; N, 6.42; found C, 57.72; H, 4.28; N, 6.55.

#### 1-[(4-Nitrophenyl)carbamoyl]cyclohexyl-4-methylbenzoate (**7**)

Yield 68%; off white powder; Mp= 201-203°C;  $R_f$  0.72 (EtOAc - petroleum ether, 1:2); IR:  $\nu_{\text{max}}/\text{cm}^{-1}$  3285 (NH), 1704 (*br*, CO, OCN);  $^1\text{H NMR}$  (500 MHz,  $\text{DMSO-}d_6$ )  $\delta_{\text{H}}$ : 10.21 (s, 1H, NH), 8.18 (d,  $J = 9$  Hz, 2H, Ar-H), 7.92 (d,  $J = 7.5$  Hz, 2H, Ar-H), 7.88 (d,  $J = 10$  Hz, 2H, Ar-H), 7.36 (d,  $J = 8$  Hz, 2H, Ar-H), 2.38 (s, 3H,  $\text{CH}_3$ ), 2.29 (d,  $J = 14$  Hz, 2H, Cyclohex-H), 1.87 (td,  $J = 13, 2.5$  Hz, 2H, Cyclohex-H), 1.67 (d,  $J = 10.5$  Hz, 3H, Cyclohex-H), 1.60 - 1.53 (m, 2H, Cyclohex-H), 1.35 - 1.29 (m, 1H, Cyclohex-H);  $^{13}\text{C NMR}$  (125 MHz,  $\text{DMSO-}d_6$ )  $\delta_{\text{C}}$ : 171.7(NH-C=O), 164.4 (O-C=O), 145.2, 144.0, 142.2, 129.6, 129.3, 127.0, 124.6, 119.7 (Ar-

C), 81.3 (O-C-C=O), 31.3, 24.5, 21.2, 21.0 (CH<sub>3</sub>, Cyclohex-C); EI-MS,  $m/z$  [M]<sup>+</sup> calcd for [C<sub>21</sub>H<sub>22</sub>N<sub>2</sub>O<sub>5</sub>]<sup>+</sup>: 382.15, found 382.21; Anal. calcd. for C<sub>21</sub>H<sub>22</sub>N<sub>2</sub>O<sub>5</sub>: C, 65.96; H, 5.80; N, 7.33; found C, 65.81; H, 5.68; N, 7.32.

### 1-[(4-Nitrophenyl)carbamoyl]cyclohexyl-4-chlorobenzoate (8)

Yield 50%; off white powder; Mp= 239-241°C; R<sub>f</sub> 0.77 (EtOAc - petroleum ether, 1:2); IR:  $\nu_{\max}/\text{cm}^{-1}$  3284 (NH), 1714 (CO), 1692 (OCN); <sup>1</sup>H NMR (500 MHz, DMSO-*d*<sub>6</sub>)  $\delta_{\text{H}}$ : 10.21 (s, 1H, NH), 8.16 (d,  $J$  = 9.2 Hz, 2H, Ar-H), 8.01 (d,  $J$  = 8.4 Hz, 2H, Ar-H), 7.86 (d,  $J$  = 9.1 Hz, 2H, Ar-H), 7.61 (d,  $J$  = 8.4 Hz, 2H, Ar-H), 2.27 (d,  $J$  = 13 Hz, 2H, Cyclohex-H), 1.87 (dist.t,  $J$  = 13, 11.4 Hz, 2H, Cyclohex-H), 1.64 (s, 3H, Cyclohex-H), 1.58 – 1.51 (m, 2H, Cyclohex-H), 1.34 – 1.27 (m, 1H, Cyclohex-H); <sup>13</sup>C NMR (125 MHz, DMSO-*d*<sub>6</sub>)  $\delta_{\text{C}}$ : 172.0 (NH-C=O), 164.2 (O-C=O), 145.6, 142.8, 139.1 (C-Cl), 132.0, 131.8, 129.0, 125.3, 120.2 (Ar-C), 82.5 (O=C-C-O), 31.9, 25.1, 21.6 (Cyclohex-C); EI-MS,  $m/z$  [M]<sup>+</sup> calcd for [C<sub>20</sub>H<sub>19</sub>ClN<sub>2</sub>O<sub>5</sub>]<sup>+</sup>: 402.09, found 402.87; Anal. calcd. for C<sub>20</sub>H<sub>19</sub>ClN<sub>2</sub>O<sub>5</sub>: C, 59.63; H, 4.75; N, 6.95; found C, 59.71; H, 4.66; N, 6.86.

### 1-[(4-Nitrophenyl)carbamoyl]cyclohexyl-4-methoxybenzoate (9)

Yield 43%; pale yellow powder; Mp= 186-189°C; R<sub>f</sub> 0.66 (EtOAc - petroleum ether, 1:2); IR:  $\nu_{\max}/\text{cm}^{-1}$  3328 (NH), 1703 (*br*, CO, OCN); <sup>1</sup>H NMR (500 MHz, DMSO-*d*<sub>6</sub>)  $\delta_{\text{H}}$ : 10.20 (s, 1H, NH), 8.17 (d,  $J$  = 10 Hz, 2H, Ar-H), 7.98 (d,  $J$  = 9 Hz, 2H, Ar-H), 7.88 (d,  $J$  = 10 Hz, 2H, Ar-H), 7.07 (d,  $J$  = 9 Hz, 2H, Ar-H), 3.83 (s, 3H, OCH<sub>3</sub>), 2.28 (d,  $J$  = 15 Hz, 2H, Cyclohex-H), 1.85 (td,  $J$  = 13.5, 3 Hz, 2H, Cyclohex-H), 1.67 (bd,  $J$  = 10.5 Hz, 3H, Cyclohex-H), 1.60 – 1.52 (m, 2H, Cyclohex-H), 1.35 – 1.28 (m, 1H, Cyclohex-H); <sup>13</sup>C NMR (125 MHz, DMSO-*d*<sub>6</sub>)  $\delta_{\text{C}}$ : 171.9 (NH-C=O), 164.1 (O-C=O), 163.4 (C-OCH<sub>3</sub>), 145.3, 142.2, 131.7, 124.6, 121.9, 119.6, 114.0 (Ar-C), 81.1 (O-C-C=O), 55.5 (OCH<sub>3</sub>), 31.3, 24.5, 21.1 (Cyclohex-C); EI-MS,  $m/z$  [M]<sup>+</sup> calcd for [C<sub>21</sub>H<sub>22</sub>N<sub>2</sub>O<sub>6</sub>]<sup>+</sup>: 398.14, found 398.59; Anal. calcd. for C<sub>21</sub>H<sub>22</sub>N<sub>2</sub>O<sub>6</sub>: C, 63.31; H, 5.57; N, 7.03; found C, 63.40; H, 5.47; N, 7.22.

### 1-[(4-Nitrophenyl)carbamoyl]cyclohexyl-2-methylbenzoate (10)

Yield 67%; off white powder; Mp= 162-165°C; R<sub>f</sub> 0.74 (EtOAc - petroleum ether, 1:2); IR:  $\nu_{\max}/\text{cm}^{-1}$  3375 (NH), 1713 (*br*, CO, OCN); <sup>1</sup>H NMR (500 MHz, DMSO-*d*<sub>6</sub>)  $\delta_{\text{H}}$ : 10.28 (bs, 1H, NH), 8.18 (d,  $J$  = 10 Hz, 2H, Ar-H), 7.95 (d,  $J$  = 8 Hz, 1H, Ar-H), 7.90 (d,  $J$  = 9 Hz, 2H, Ar-H), 7.50 (t,  $J$  = 7.5 Hz, 1H, Ar-H), 7.38 – 7.32 (m, 2H, Ar-H), 2.41 (s, 3H, CH<sub>3</sub>), 2.28 (d,  $J$  = 14 Hz, 2H, Cyclohex-H), 1.89 (td,  $J$  = 14.2, 3.5 Hz, 2H, Cyclohex-H), 1.69 (d,  $J$  = 10.5 Hz, 3H, Cyclohex-H), 1.64 – 1.56 (m, 2H, Cyclohex-H), 1.36 – 1.29 (m, 1H, Cyclohex-H); <sup>13</sup>C NMR (125 MHz, DMSO-*d*<sub>6</sub>)  $\delta_{\text{C}}$ : 171.9 (NH-C=O), 165.7 (O-C=O), 142.1, 139.2, 132.3, 131.5, 130.1, 129.8, 126.0, 124.7, 119.7 (Ar-C), 81.8 (O-C-C=O), 31.3, 24.5, 21.1 (Cyclohex-C, CH<sub>3</sub>), 20.8; EI-MS,  $m/z$  [M]<sup>+</sup> calcd for [C<sub>21</sub>H<sub>22</sub>N<sub>2</sub>O<sub>5</sub>]<sup>+</sup>: 382.15, found 382.47; Anal. calcd. for C<sub>21</sub>H<sub>22</sub>N<sub>2</sub>O<sub>5</sub>: C, 65.96; H, 5.80; N, 7.33; found C, 65.87; H, 5.78; N, 7.32.

**1-[(4-Nitrophenyl)carbamoyl]cyclohexyl-4-bromobenzoate (11)**

Yield 62%; off white powder; Mp= 243-245°C; R<sub>f</sub> 0.61 (EtOAc - petroleum ether, 1:2); IR:  $\nu_{\max}/\text{cm}^{-1}$  3282 (NH), 1713 (CO), 1686 (OCN); <sup>1</sup>H NMR (500 MHz, DMSO-*d*<sub>6</sub>)  $\delta_{\text{H}}$ : 10.24 (s, 1H, NH), 8.18 (d, *J* = 9 Hz, 2H, Ar-H), 7.95 (d, *J* = 8 Hz, 2H, Ar-H), 7.87 (d, *J* = 9 Hz, 2H, Ar-H), 7.78 (d, *J* = 8.5 Hz, 2H, Ar-H), 2.29 (d, *J* = 14 Hz, 2H, Cyclohex-H), 1.89 (td, *J* = 13.5, 3 Hz, 2H, Cyclohex-H), 1.67 (d, *J* = 10 Hz, 3H, Cyclohex-H), 1.59 – 1.54 (m, 2H, Cyclohex-H), 1.36 – 1.28 (m, 1H, Cyclohex-H). <sup>13</sup>C NMR (125 MHz, DMSO-*d*<sub>6</sub>)  $\delta_{\text{C}}$ : 171.4 (NH-C=O), 163.8 (O-C=O), 145.1, 142.3, 131.9, 131.5, 128.9, 127.7, 124.6, 119.8 (Ar-C), 82.0 (O-C-C=O), 31.2, 24.4, 21.0 (Cyclohex-C); EI-MS, *m/z* [M]<sup>+</sup> calcd for [C<sub>20</sub>H<sub>19</sub>BrN<sub>2</sub>O<sub>5</sub>]<sup>+</sup>: 446.04, found 446.12; Anal. calcd. for C<sub>20</sub>H<sub>19</sub>BrN<sub>2</sub>O<sub>5</sub>: C, 53.71; H, 4.28; N, 6.26; found C, 53.65; H, 4.13; N, 6.19.

**1-[(4-Nitrophenyl)carbamoyl]cyclohexyl-2-iodobenzoate (12)**

Yield 42%; off white powder; Mp= 136-139°C; R<sub>f</sub> 0.70 (EtOAc - petroleum ether, 1:2); IR:  $\nu_{\max}/\text{cm}^{-1}$  3352 (NH), 1717 (*br*, CO, OCN); <sup>1</sup>H NMR (400 MHz, DMSO-*d*<sub>6</sub>)  $\delta_{\text{H}}$ : 10.58 (s, 1H, NH), 8.49 (d, *J* = 9.6 Hz, 2H, Ar-H), 8.31 (d, *J* = 8 Hz, 1H, Ar-H), 8.23-8.19 (m, 3H, Ar-H), 7.86 (t, *J* = 8 Hz, 1H, Ar-H), 7.60 (td, *J* = 8.4, 1.2 Hz, 1H, Ar-H), 2.59 (d, *J* = 13.2 Hz, 2H, Cyclohex-H), 2.20 (td, *J* = 12.8, 4 Hz, 2H, Cyclohex-H), 1.96 – 1.91 (bs, 5H, Cyclohex-H), 1.67-1.63 (m, 1H, Cyclohex-H); <sup>13</sup>C NMR (100 MHz, DMSO-*d*<sub>6</sub>)  $\delta_{\text{C}}$ : 171.3 (O-C=O), 165.2 (NH-C=O), 145.2, 142.3, 140.8, 135.2, 133.2, 130.7, 128.3, 124.6, 119.8 (Ar-C), 94.7 (C-I), 82.7 (O=C-C-O), 31.2, 24.4, 21.0 (Cyclohex-C); EI-MS, *m/z* [M]<sup>+</sup> calcd for [C<sub>20</sub>H<sub>19</sub>IN<sub>2</sub>O<sub>5</sub>]<sup>+</sup>: 494.03, found 494.35; Anal. calcd. for C<sub>20</sub>H<sub>19</sub>IN<sub>2</sub>O<sub>5</sub>: C, 48.60; H, 3.87; N, 5.67; found C, 48.57; H, 3.65; N, 5.55.

**1-[(4-Nitrophenyl)carbamoyl]cyclohexyl-4-nitrobenzoate (13)**

Yield 71%; pale yellow powder; Mp= 234-236°C; R<sub>f</sub> 0.72 (EtOAc - petroleum ether, 1:2); IR:  $\nu_{\max}/\text{cm}^{-1}$  3379 (NH), 1722 (*br*, CO, OCN); <sup>1</sup>H NMR (500 MHz, DMSO-*d*<sub>6</sub>)  $\delta_{\text{H}}$ : 10.37 (bs, 1H, NH), 8.38 (d, *J* = 9 Hz, 2H, Ar-H), 8.27 (d, *J* = 9 Hz, 2H, Ar-H), 8.18 (d, *J* = 9 Hz, 2H, Ar-H), 7.86 (d, *J* = 9.5 Hz, 2H, Ar-H), 2.31 (d, *J* = 13.5 Hz, 2H, Cyclohex-H), 1.93 (td, *J* = 13.5, 2.5 Hz, 2H, Cyclohex-H), 1.68 (bs, 3H, Cyclohex-H), 1.62 – 1.54 (m, 2H, Cyclohex-H), 1.38 – 1.30 (m, 1H, Cyclohex-H); <sup>13</sup>C NMR (125 MHz, DMSO-*d*<sub>6</sub>)  $\delta_{\text{C}}$ : 171.1 (NH-C=O), 163.0 (O-C=O), 150.4, 145.0, 142.4, 135.1, 131.0, 124.6, 123.9, 119.8 (Ar-C), 82.7 (O=C-C-O), 31.2, 24.4, 21.0 (Cyclohex-C); EI-MS, *m/z* [M]<sup>+</sup> calcd for [C<sub>20</sub>H<sub>19</sub>N<sub>3</sub>O<sub>7</sub>]<sup>+</sup>: 413.12, found 413.16; Anal. calcd. for C<sub>20</sub>H<sub>19</sub>N<sub>3</sub>O<sub>7</sub>: C, 58.11; H, 4.63; N, 10.16; found C, 58.06; H, 4.69; N, 9.87.

**1-[(4-Nitrophenyl)carbamoyl]cyclohexyl-2-nitrobenzoate (14)**

Yield 57%; white powder; Mp= 200-204°C; R<sub>f</sub> 0.65 (EtOAc - petroleum ether, 1:2); IR:  $\nu_{\max}/\text{cm}^{-1}$  3379 (NH), 1731 (CO), 1696 (OCN); <sup>1</sup>H NMR (500 MHz, DMSO-*d*<sub>6</sub>)  $\delta_{\text{H}}$ : 10.25 (s, 1H, NH), 8.19 (d, *J* = 8.4 Hz, 2H, Ar-H), 8.03 (d, *J* = 7.6 Hz, 1H, Ar-H), 7.97 (d, *J* = 7.6 Hz, 1H, Ar-H), 7.90 – 7.81 (m, 4H, Ar-H), 2.27 (d, *J* = 13.7 Hz, 2H, Cyclohex-H), 1.92 (t, *J* = 12.2 Hz, 2H, Cyclohex-H), 1.64 - 1.53 (m, 5H, Cyclohex-H), 1.33 - 1.31 (m, *J* = 9.1 Hz, 1H,

Cyclohex-**H**);  $^{13}\text{C}$  NMR (125 MHz, DMSO- $d_6$ )  $\delta_{\text{C}}$ : 171.2 (NH-C=O), 163.9 (O-C=O), 148.8, 145.6, 143.0, 133.9, 130.9, 126.4, 125.2, 124.7, 120.4, 120.2 (Ar-C), 84.5 (O=C-C-O), 31.7, 24.9, 21.4 (Cyclohex-C); EI-MS,  $m/z$   $[\text{M}]^+$  calcd for  $[\text{C}_{20}\text{H}_{19}\text{N}_3\text{O}_7]^+$ : 413.12, found 413.05; Anal. calcd. for  $\text{C}_{20}\text{H}_{19}\text{N}_3\text{O}_7$ : C, 58.11; H, 4.63; N, 10.16; found C, 57.98; H, 4.55; N, 10.19.

### Ethyl [1-[(4-nitrophenyl)carbamoyl]cyclohexyl] phthalate (15)

Yield 48%; Off white powder; Mp= 179-181°C;  $R_f$  0.62 (EtOAc - petroleum ether, 1:2); IR:  $\nu_{\text{max}}/\text{cm}^{-1}$  3358 (NH), 1740 (CO), 1698 (OCN);  $^1\text{H}$  NMR (400 MHz, DMSO- $d_6$ )  $\delta_{\text{H}}$ : 10.14 (s, 1H, NH), 8.21 (d,  $J$  = 8.8 Hz, 2H, Ar-H), 7.98 – 7.90 (m, 3H, Ar-H), 7.71 (s, 3H, Ar-H), 4.14 (q,  $J$  = 7.2 Hz, 2H, CH<sub>2</sub>), 2.29 (d,  $J$  = 14 Hz, 2H, Cyclohex-H), 1.91 (td,  $J$  = 13, 2.8 Hz, 2H, Cyclohex-H), 1.67-1.55 (m, 5H, Cyclohex-H), 1.34-1.31 (m, 1H, Cyclohex-H), 1.10 (t,  $J$  = 7.2 Hz, 2H, CH<sub>3</sub>);  $^{13}\text{C}$  NMR (100 MHz, DMSO- $d_6$ )  $\delta_{\text{C}}$ : 171.1 (NH-C=O), 167.3 (CH<sub>2</sub>-O-C=O), 165.1 (O-C=O), 145.1, 142.3, 132.5, 132.1, 131.4, 130.7, 129.4, 128.7, 124.7, 119.6, (Ar-C), 82.7 (O-C-C=O), 61.5 (CH<sub>2</sub>), 31.2, 24.0, 20.9, 13.6 (Cyclohex-C, CH<sub>3</sub>); EI-MS,  $m/z$   $[\text{M}]^+$  calcd for  $[\text{C}_{23}\text{H}_{24}\text{N}_2\text{O}_7]^+$ : 440.15, found 440.86; Anal. calcd. for  $\text{C}_{23}\text{H}_{24}\text{N}_2\text{O}_7$ : C, 62.72; H, 5.49; N, 6.36; found C, 62.66; H, 5.36; N, 6.12.

### 1-[(4-Nitrophenyl)carbamoyl]cyclohexyl cinnamate (16)

Yield 54%; off white powder; Mp= 184-186°C;  $R_f$  0.59 (EtOAc - petroleum ether, 1:2); IR:  $\nu_{\text{max}}/\text{cm}^{-1}$  3285 (NH), 1700 (CO), 1632 (OCN);  $^1\text{H}$  NMR (500 MHz, DMSO- $d_6$ )  $\delta_{\text{H}}$ : 10.23 (s, 1H, NH), 8.17 (d,  $J$  = 9 Hz, 2H, Ar-H), 7.89 (d,  $J$  = 8.5 Hz, 2H, Ar-H), 7.74 – 7.73 (m, 2H, Ar-H), 7.68 (d,  $J$  = 15.5 Hz, 1H, OCO-CH=CH), 7.44 – 7.43 (m, 3H, Ar-H), 6.72 (d,  $J$  = 15.5 Hz, 1H, OCO-CH=CH), 2.22 (d,  $J$  = 13 Hz, 2H, Cyclohex-H), 1.84 (t,  $J$  = 12 Hz, 2H, Cyclohex-H), 1.65 – 1.56 (m, 5H, Cyclohex-H), 1.32 – 1.30 (m, 1H, Cyclohex-H);  $^{13}\text{C}$  NMR (125 MHz, DMSO- $d_6$ )  $\delta_{\text{C}}$ : 171.9 (NH-C=O), 165.0 (O-C=O), 145.4 (Ar-C), 145.1 (OCO-CH=CH), 142.2, 133.9, 130.6, 129.0, 128.4, 124.6, 119.6 (Ar-C), 118.1 (OCO-CH=CH), 81.1 (O-C-C=O), 31.3, 24.5, 20.9 (Cyclohex-C); EI-MS,  $m/z$   $[\text{M}]^+$  calcd for  $[\text{C}_{22}\text{H}_{22}\text{N}_2\text{O}_5]^+$ : 394.15, found 394.93; Anal. calcd. for  $\text{C}_{22}\text{H}_{22}\text{N}_2\text{O}_5$ : C, 66.99; H, 5.62; N, 7.10; found C, 66.96; H, 5.54; N, 6.97.

### 1-[(4-Nitrophenyl)carbamoyl]cyclohexyl benzoate (17)

Yield 65%; off white powder; Mp= 186-189°C;  $R_f$  0.65 (EtOAc - petroleum ether, 1:2); IR:  $\nu_{\text{max}}/\text{cm}^{-1}$  3285 (NH), 1704 (br, CO, OCN);  $^1\text{H}$  NMR (500 MHz, DMSO- $d_6$ )  $\delta_{\text{H}}$ : 10.23 (s, 1H, NH), 8.18 (d,  $J$  = 10 Hz, 2H, Ar-H), 8.03 (d,  $J$  = 8 Hz, 2H, Ar-H), 7.88 (d,  $J$  = 9.5 Hz, 2H, Ar-H), 7.69 (t,  $J$  = 7.5 Hz, 1H, Ar-H), 7.56 (t,  $J$  = 7.5 Hz, 2H, Ar-H), 2.30 (d,  $J$  = 14 Hz, 2H, Cyclohex-H), 1.88 (td,  $J$  = 13.5, 3.5 Hz, 2H, Cyclohex-H), 1.68 (bd,  $J$  = 10.5 Hz, 3H, Cyclohex-H), 1.62 – 1.54 (m, 2H, Cyclohex-H), 1.36 – 1.29 (m, 1H, Cyclohex-H);  $^{13}\text{C}$  NMR (125 MHz, DMSO- $d_6$ )  $\delta_{\text{C}}$ : 171.6 (NH-C=O), 164.5 (O-C=O), 145.2, 142.3, 133.6, 129.7, 129.5, 128.8, 124.6, 119.7 (Ar-C), 81.6 (O-C-C=O), 31.3, 24.5, 21.0 (Cyclohex-C); EI-MS,  $m/z$   $[\text{M}]^+$  calcd for  $[\text{C}_{20}\text{H}_{20}\text{N}_2\text{O}_5]^+$ : 368.13, found 368.27; Anal. calcd. for  $\text{C}_{20}\text{H}_{20}\text{N}_2\text{O}_5$ : C, 65.21; H, 5.47; N, 7.60; found C, 64.99; H, 5.39; N, 7.55.

### 5.1.3. General method B for Passerini reactions

*p*-Nitrophenyl isocyanide (50 mg, 0.337 mmol, 0.5 eq) was added to a mixture of cyclohexanone (3.37 mmol, 5 eq), and the appropriate carboxylic acid (0.674 mmol, 1 eq). The mixture was stirred at room temperature for 24 hours. The reaction was monitored by TLC. After the reaction completion, the reaction was quenched by adding DCM (5 mL) and neutralized with saturated solution of NaHCO<sub>3</sub>, then the mixture was washed with DCM (3 × 10 mL). The organic layers were combined, dried over anhydrous sodium sulfate and evaporated under reduced pressure [31]. The crude product was recrystallized from a mixture of DCM/petroleum ether (1:1).

#### 1-[(4-Nitrophenyl)carbamoyl]cyclohexyl formate (18)

Yield 89%; pale yellow powder; Mp= 162-165°C; R<sub>f</sub> 0.60 (EtOAc - petroleum ether, 1:2); IR:  $\nu_{\max}/\text{cm}^{-1}$  3383 (NH), 1705 (*br*, CO, OCN); <sup>1</sup>H NMR (500 MHz, DMSO-*d*<sub>6</sub>)  $\delta_{\text{H}}$ : 10.26 (s, 1H, NH), 8.30 (s, 1H, O=CH), 8.19 (d, *J* = 9.5 Hz, 2H, Ar-H), 7.90 (d, *J* = 9.5 Hz, 2H, Ar-H), 2.15 (d, *J* = 16 Hz, 2H, Cyclohex-H), 1.84 (dist.t, *J* = 12.5, 11 Hz, 2H, Cyclohex-H), 1.62 (d, *J* = 10 Hz, 3H, Cyclohex-H), 1.53 – 1.46 (m, 2H, Cyclohex-H), 1.33 – 1.25 (m, 1H, Cyclohex-H); <sup>13</sup>C NMR (125 MHz, DMSO-*d*<sub>6</sub>)  $\delta_{\text{C}}$ : 171.3 (NH-C=O), 161.1 (O-C=O), 145.1, 142.4, 124.6, 119.7 (Ar-C) 81.5 (O-C-C=O), 31.3, 24.3, 20.6 (Cyclohex-C); EI-MS, *m/z* [M]<sup>+</sup> calcd for [C<sub>14</sub>H<sub>16</sub>N<sub>2</sub>O<sub>5</sub>]<sup>+</sup>: 292.10, found 292.15; Anal. calcd. for C<sub>14</sub>H<sub>16</sub>N<sub>2</sub>O<sub>5</sub>: C, 57.53; H, 5.52; N, 9.58; found C, 57.65; H, 5.45; N, 9.60.

#### 1-[(4-Nitrophenyl)carbamoyl]cyclohexyl acetate (19)

Yield 77%; pale yellow powder; Mp= 143-145°C; R<sub>f</sub> 0.58 (EtOAc - petroleum ether, 1:2); IR:  $\nu_{\max}/\text{cm}^{-1}$  3446 (NH), 1720 (CO), 1629 (OCN); <sup>1</sup>H NMR (500 MHz, DMSO-*d*<sub>6</sub>)  $\delta_{\text{H}}$ : 10.15 (s, 1H, NH), 8.18 (d, *J* = 9 Hz, 2H, Ar-H), 7.89 (d, *J* = 9 Hz, 2H, Ar-H), 2.14 (bs, 1H, Cyclohex-H), 2.11 (s, 4H, Cyclohex-H, CH<sub>3</sub>), 1.76 (td, *J* = 13.5, 3 Hz, 2H, Cyclohex-H), 1.60 (d, *J* = 9.5 Hz, 3H, Cyclohex-H), 1.53 – 1.45 (m, 2H, Cyclohex-H), 1.31 – 1.22 (m, 1H, Cyclohex-H); <sup>13</sup>C NMR (125 MHz, DMSO-*d*<sub>6</sub>)  $\delta_{\text{C}}$ : 171.8 (NH-C=O), 169.6 (O-C=O), 145.2, 142.2, 124.6, 119.6 (Ar-C), 80.9 (O-C-C=O), 31.2, 24.5, 21.2, 20.8 (Cyclohex-C, CH<sub>3</sub>); EI-MS, *m/z* [M]<sup>+</sup> calcd for [C<sub>15</sub>H<sub>18</sub>N<sub>2</sub>O<sub>5</sub>]<sup>+</sup>: 306.12, found 306.22; Anal. calcd. for C<sub>15</sub>H<sub>18</sub>N<sub>2</sub>O<sub>5</sub>: C, 58.82; H, 5.92; N, 9.15; found C, 58.72; H, 5.83; N, 8.88.

#### 1-[(4-Nitrophenyl)carbamoyl]cyclohexyl propionate (20)

Yield 74%; Yellow powder; Mp= 147-150°C; R<sub>f</sub> 0.66 (EtOAc - petroleum ether, 1:2); IR:  $\nu_{\max}/\text{cm}^{-1}$  3396 (NH), 1719 (*br*, CO, OCN); <sup>1</sup>H NMR (500 MHz, DMSO-*d*<sub>6</sub>)  $\delta_{\text{H}}$ : 10.13 (s, 1H, NH), 8.18 (d, *J* = 9 Hz, 2H, Ar-H), 7.89 (d, *J* = 9.5 Hz, 2H, Ar-H), 2.43 (q, *J* = 7.5, 8 Hz, 2H, OCOCH<sub>2</sub>), 2.13 (d, *J* = 13.5 Hz, 2H, Cyclohex-H), 1.77 (td, *J* = 13.5, 2.5 Hz, 2H, Cyclohex-H), 1.60 (d, *J* = 10 Hz, 3H, Cyclohex-H), 1.52 – 1.44 (m, 2H, Cyclohex-H), 1.29 – 1.22 (m, 1H, Cyclohex-H), 1.03 (t, *J* = 7.5 Hz, 3H, CH<sub>3</sub>); <sup>13</sup>C NMR (125 MHz, DMSO-*d*<sub>6</sub>)  $\delta_{\text{C}}$ : 172.7 (NH-C=O), 171.9 (O-C=O), 145.3, 142.2, 124.6, 119.6 (Ar-C), 80.7 (O-C-C=O), 31.2, 27.2, 24.5, 20.8, 9.0 (Cyclohex-C, CH<sub>2</sub>, CH<sub>3</sub>); EI-MS, *m/z* [M]<sup>+</sup> calcd for [C<sub>16</sub>H<sub>20</sub>N<sub>2</sub>O<sub>5</sub>]<sup>+</sup>: 320.13,

found 320.30; Anal. calcd. for C<sub>16</sub>H<sub>20</sub>N<sub>2</sub>O<sub>5</sub>: C, 59.99; H, 6.29; N, 8.74; found C, 59.76; H, 6.13; N, 8.55.

### 1-[(4-Nitrophenyl)carbamoyl]cyclohexyl-2-hydroxy-2-phenylacetate (21)

Yield 75%; pale yellow powder; Mp= 179-182°C; R<sub>f</sub> 0.68 (EtOAc - petroleum ether, 1:2); IR:  $\nu_{\max}/\text{cm}^{-1}$  3463 (OH), 3378 (NH), 1728 (CO), 1692 (OCN); <sup>1</sup>H NMR (500 MHz, DMSO-*d*<sub>6</sub>)  $\delta_{\text{H}}$ : 10.08 (s, 1H, NH), 8.21 (d, *J* = 9 Hz, 2H, Ar-H), 7.88 (d, *J* = 9.5 Hz, 2H, Ar-H), 7.45 (d, *J* = 7.5 Hz, 2H, Ar-H), 7.37 (t, *J* = 7.5 Hz, 2H, Ar-H), 7.33 – 7.30 (m, 1H, Ar-H), 6.14 (d, *J* = 4.5 Hz, 1H, Ph-CH), 5.27 (d, *J* = 3 Hz, 1H, OH), 2.08 – 2.03 (m, 2H, Cyclohex-H), 1.73 (td, *J* = 14, 4 Hz, 1H, Cyclohex-H), 1.57 (td, *J* = 12.5, 4 Hz, 1H, Cyclohex-H), 1.49 – 1.46 (m, 1H, Cyclohex-H), 1.36 – 1.28 (m, 2H, Cyclohex-H), 1.24 – 1.21 (m, 1H, Cyclohex-H), 1.12 – 1.04 (m, 1H, Cyclohex-H), 0.53 – 0.45 (m, 1H, Cyclohex-H); <sup>13</sup>C NMR (125 MHz, DMSO-*d*<sub>6</sub>)  $\delta_{\text{C}}$ : 171.5 (O-C=O), 171.3 (NH-C=O), 145.1, 142.3, 139.7, 128.2, 128.0, 126.9, 124.6, 119.7 (Ar-C), 81.4 (O-C-C=O), 72.4 (CHOH), 33.0, 28.8, 24.2, 20.5, 19.8 (Cyclohex-C); EI-MS, *m/z* [M]<sup>+</sup> calcd for [C<sub>21</sub>H<sub>22</sub>N<sub>2</sub>O<sub>6</sub>]<sup>+</sup>: 398.14, found 398.53; Anal. calcd. for C<sub>21</sub>H<sub>22</sub>N<sub>2</sub>O<sub>6</sub>: C, 63.31; H, 5.57; N, 7.03; found C, 63.34; H, 5.66; N, 7.10.

### 1-[(4-Nitrophenyl)carbamoyl]cyclohexyl-2-phenylacetate (22)

Yield 69%; Yellow crystals; Mp= 74-76°C; R<sub>f</sub> 0.65 (EtOAc - petroleum ether, 1:2); IR:  $\nu_{\max}/\text{cm}^{-1}$  3337 (NH), 1741 (CO), 1690 (OCN); <sup>1</sup>H NMR (500 MHz, DMSO-*d*<sub>6</sub>)  $\delta_{\text{H}}$ : 10.20 (s, 1H, NH), 8.19 (d, *J* = 9 Hz, 2H, Ar-H), 7.90 (d, *J* = 9.5 Hz, 2H, Ar-H), 7.32 – 7.22 (m, 5H, Ar-H), 3.78 (s, 2H, Ph-CH<sub>2</sub>), 2.12 (d, *J* = 13.5 Hz, 2H, Cyclohex-H), 1.74 (td, *J* = 14, 3.5 Hz, 2H, Cyclohex-H), 1.52 (d, *J* = 10.5 Hz, 3H, Cyclohex-H), 1.40 – 1.28 (m, 2H, Cyclohex-H), 1.25 – 1.20 (m, 1H, Cyclohex-H); <sup>13</sup>C NMR (125 MHz, DMSO-*d*<sub>6</sub>)  $\delta_{\text{C}}$ : 171.7 (NH-C=O), 170.2 (O-C=O), 145.2, 142.3, 134.2, 129.4, 128.3, 126.9, 124.6, 119.6 (Ar-C), 81.3 (O-C-C=O), 40.7 (CH<sub>2</sub>), 31.1, 26.4, 24.4, 20.6 (Cyclohex-C); EI-MS, *m/z* [M]<sup>+</sup> calcd for [C<sub>21</sub>H<sub>22</sub>N<sub>2</sub>O<sub>5</sub>]<sup>+</sup>: 382.15, found 382.33; Anal. calcd. for C<sub>21</sub>H<sub>22</sub>N<sub>2</sub>O<sub>5</sub>: C, 65.96; H, 5.80; N, 7.33; found C, 65.45; H, 5.79; N, 7.30.

### 1-[(4-Nitrophenyl)carbamoyl]cyclohexyl-2-acetoxybenzoate (23)

Yield 80%; white powder; Mp= 136-138°C; R<sub>f</sub> 0.63 (EtOAc - petroleum ether, 1:2); IR:  $\nu_{\max}/\text{cm}^{-1}$  3371 (NH), 1766 (CO), 1726 (CO), 1682 (OCN); <sup>1</sup>H NMR (500 MHz, DMSO-*d*<sub>6</sub>)  $\delta_{\text{H}}$ : 10.16 (s, 1H, NH), 8.19 (d, *J* = 10 Hz, 2H, Ar-H), 8.09 (dd, *J* = 7.5, 2 Hz, 1H, Ar-H), 7.87 (d, *J* = 9 Hz, 2H, Ar-H), 7.70 (td, *J* = 7.5, 2 Hz, 1H, Ar-H), 7.46 (td, *J* = 7.5, 1 Hz, 1H, Ar-H), 7.24 (dd, *J* = 8, 1 Hz, 1H, Ar-H), 2.27 (d, *J* = 14 Hz, 2H, Cyclohex-H), 2.02 (s, 3H, CH<sub>3</sub>), 1.87 (td, *J* = 14, 3.5 Hz, 2H, Cyclohex-H), 1.67 – 1.66 (m, 3H, Cyclohex-H), 1.60 – 1.53 (m, 2H, Cyclohex-H), 1.36 – 1.28 (m, 1H, Cyclohex-H); <sup>13</sup>C NMR (125 MHz, DMSO-*d*<sub>6</sub>)  $\delta_{\text{C}}$ : 171.3 (NH-C=O), 168.9 (O-CO-CH<sub>3</sub>), 162.7 (O-C=O), 150.0, 145.2, 142.3, 134.3, 131.1, 126.2, 124.6, 123.9, 123.4, 119.8 (Ar-C), 82.1 (O-C-C=O), 31.1, 24.4, 20.9, 20.5 (CH<sub>3</sub>, Cyclohex-C); EI-MS, *m/z* [M]<sup>+</sup> calcd for [C<sub>22</sub>H<sub>22</sub>N<sub>2</sub>O<sub>7</sub>]<sup>+</sup>: 426.14, found 426.64; Anal. calcd. for C<sub>22</sub>H<sub>22</sub>N<sub>2</sub>O<sub>7</sub>: C, 61.97; H, 5.20; N, 6.57; found C, 61.89; H, 5.19; N, 6.47.

**Bis[1-[(4-nitrophenyl)carbamoyl]cyclohexyl] succinate (24)**

Yield 72%; Yellow crystals; Mp= 196-199°C; R<sub>f</sub> 0.66 (EtOAc - petroleum ether, 1:2); IR:  $\nu_{\max}/\text{cm}^{-1}$  3363 (NH), 1733 (CO), 1700 (OCN); <sup>1</sup>H NMR (500 MHz, DMSO-*d*<sub>6</sub>)  $\delta_{\text{H}}$ : 10.00 (s, 2H, 2 NH), 8.14 (d, *J* = 9.5 Hz, 4H, Ar-H), 7.84 (d, *J* = 9 Hz, 4H, Ar-H), 2.72 (bs, 4H, 2 CH<sub>2</sub>), 2.06 (d, *J* = 13.5 Hz, 4H, Cyclohex-H), 1.72 (td, *J* = 14, 3.5 Hz, 4H, Cyclohex-H), 1.59 – 1.42 (m, 10H, Cyclohex-H), 1.26 – 1.22 (m, 2H, Cyclohex-H); <sup>13</sup>C NMR (125 MHz, DMSO-*d*<sub>6</sub>)  $\delta_{\text{C}}$ : 171.5 (2 NH-C=O), 171.2 (2 O-C=O), 145.1, 142.2, 124.5, 119.6 (Ar-C), 81.4 (2 O-C-C=O), 31.1, 29.0, 24.4, 20.7 (CH<sub>2</sub>, Cyclohex-C); EI-MS, *m/z* [M]<sup>+</sup> calcd for [C<sub>30</sub>H<sub>34</sub>N<sub>4</sub>O<sub>10</sub>]<sup>+</sup>: 610.22, found 610.47; Anal. calcd. for C<sub>30</sub>H<sub>34</sub>N<sub>4</sub>O<sub>10</sub>: C, 59.01; H, 5.61; N, 9.18; found C, 59.11; H, 5.58; N, 9.12.

**Synthesis of 1-Hydroxy-N-(4-nitrophenyl)cyclohexanecarboxamide (25b)**

*p*-Nitrophenyl isocyanide (50 mg, 0.337 mmol, 0.5 eq) was added to a mixture of cyclohexanone (331 mg, 3.37 mmol, 5 eq), and trifluoroacetic acid (154 mg, 1.35 mmol, 2 eq). The mixture was stirred at room temperature for 24 hours. The reaction was monitored by TLC. After the reaction completion, the reaction was quenched by adding DCM (5 mL) and neutralized with saturated solution of NaHCO<sub>3</sub>, then the mixture was washed with DCM (3 × 10 mL). The organic layers were combined, dried over anhydrous sodium sulfate and evaporated under reduced pressure [31]. The crude product was recrystallized from a mixture of DCM/petroleum ether (1:2). Yield 79%; yellow powder; Mp= 70-73°C; R<sub>f</sub> 0.64 (EtOAc - petroleum ether, 1:2); IR:  $\nu_{\max}/\text{cm}^{-1}$  3320 (OH), 3284 (NH), 1688 (OCN); <sup>1</sup>H NMR (500 MHz, DMSO-*d*<sub>6</sub>)  $\delta_{\text{H}}$ : 10.28 (s, 1H, NH), 8.19 (d, *J* = 9.5 Hz, 2H, Ar-H), 8.04 (d, *J* = 9.5 Hz, 2H, Ar-H), 5.58 (s, 1H, OH), 1.72 (td, *J* = 13, 3.5 Hz, 2H, Cyclohex-H), 1.63 – 1.58 (m, 5H, Cyclohex-H), 1.52 – 1.49 (m, 2H, Cyclohex-H), 1.22 – 1.17 (m, 1H, Cyclohex-H); <sup>13</sup>C NMR (125 MHz, DMSO-*d*<sub>6</sub>)  $\delta_{\text{C}}$ : 177.1 (NH-C=O), 145.2, 142.2, 124.6, 119.3 (Ar-C), 74.0 (HO-C-C=O), 33.6, 24.9, 20.7 (Cyclohex-C); EI-MS, *m/z* [M]<sup>+</sup> calcd for [C<sub>13</sub>H<sub>16</sub>N<sub>2</sub>O<sub>4</sub>]<sup>+</sup>: 264.11, found 264.61; Anal. calcd. for C<sub>13</sub>H<sub>16</sub>N<sub>2</sub>O<sub>4</sub>: C, 59.08; H, 6.10; N, 10.60; found C, 59.14; H, 5.99; N, 10.50.

**Synthesis of 3-(4-nitrophenyl)-1-oxa-3-azaspiro[4.5]decane-2,4-dione (26c)**

*p*-Nitrophenyl isocyanide (50 mg, 0.337 mmol, 0.5 eq.) was added to a mixture of cyclohexanone (331 mg, 3.37 mmol, 5 eq) and trichloroacetic acid (109.8 mg, 0.674 mmol, 1 eq). The mixture was stirred at room temperature for 24 hours. The reaction was monitored by TLC. After the reaction completion, the reaction was quenched by adding DCM (5 mL) and neutralized with a saturated solution of NaHCO<sub>3</sub>. Then the mixture was washed with DCM (3 × 10 mL). The organic layers were combined, dried over anhydrous sodium sulfate and evaporated under reduced pressure [31]. The crude product was recrystallized from a mixture of DCM/petroleum ether (1:2). Yield 86%; Yellow crystals; Mp= 180-182°C; R<sub>f</sub> 0.69 (EtOAc - petroleum ether, 1:2); IR:  $\nu_{\max}/\text{cm}^{-1}$  1814 (COO), 1734 (CO); <sup>1</sup>H NMR (500 MHz, DMSO-*d*<sub>6</sub>)  $\delta_{\text{H}}$ : 8.39 (d, *J* = 9 Hz, 2H, Ar-H), 7.81 (d, *J* = 9.5 Hz, 2H, Ar-H), 2.09 (d, *J* = 13 Hz, 2H, Cyclohex-H), 1.84 (td, *J* = 13, 4.5 Hz, 2H, Cyclohex-H), 1.76 – 1.71 (m, 2H, Cyclohex-H), 1.67 – 1.60 (m, 1H, Cyclohex-H), 1.58 – 1.50 (m, 2H, Cyclohex-H), 1.43 – 1.34 (m, 1H,

Cyclohex-**H**);  $^{13}\text{C}$  NMR (125 MHz, DMSO- $d_6$ )  $\delta_{\text{C}}$ : 173.7 (N-COC), 152.5 (N-COO), 146.6, 136.9, 127.3, 124.2 (Ar-C), 85.1 (O-C-C=O), 31.1, 23.7, 20.8 (Cyclohex-C); EI-MS,  $m/z$   $[\text{M}]^+$  calcd for  $[\text{C}_{14}\text{H}_{14}\text{N}_2\text{O}_5]^+$ : 290.09, found 290.34; Anal. calcd. for  $\text{C}_{14}\text{H}_{14}\text{N}_2\text{O}_5$ : C, 57.93; H, 4.86; N, 9.65; found C, 58.08; H, 4.89; N, 9.87.

### Synthesis of **5**, 5-Dimethyl-3-(4-nitro-phenylamino)-Cyclohex-2-enone (**30**)

*p*-Nitrophenyl isocyanide **3** (50 mg, 0.337 mmol, 1.1eq) was added to a solution of dimedone (47 mg, 0.337 mmol, 1.1 eq) and *o*-nitrobenzoic acid (51 mg, 0.307 mmol, 1eq) in a mixture of 2,2,2-trifluoroethanol (TFE) and ethanol (1:1, 2mL). The reaction mixture was stirred under Reflux for 3 days. The reaction was monitored by TLC. After the reaction completion, the mixture was evaporated and washed with a mixture of DCM/n-hexane (1:2). The crude product recrystallized from ethanol. Yield 81%; pale yellow crystals; Mp= 244-246°C; [lit.[60] Mp=246-247 °C]  $R_f$  0.36 (EtOAc - petroleum ether, 1:2); IR:  $\nu_{\text{max}}/\text{cm}^{-1}$  3256 (NH), 3062 (CH=CH);  $^1\text{H}$  NMR (500 MHz, DMSO- $d_6$ )  $\delta_{\text{H}}$ : 9.32 (s, 1H, NH), 8.20 (d,  $J = 9$  Hz, 2H, Ar-H), 7.35 (d,  $J = 7$  Hz, 2H, Ar-H), 5.66 (s, 1H, C=CH-CO), 2.42 (s, 2H, CH<sub>2</sub>), 2.11 (s, 2H, CH<sub>2</sub>), 1.02 (s, 6H, 2 CH<sub>3</sub>);  $^{13}\text{C}$  NMR (125 MHz, DMSO- $d_6$ )  $\delta_{\text{C}}$ : 196.6 (C=O), 157.4 (NH-C=CH), 146.3, 141.5, 125.3, 120.3 (Ar-C), 101.1 (C=CH-CO), 50.0 (CH<sub>2</sub>-CO), 42.1(CH<sub>2</sub>-C-(CH<sub>3</sub>)<sub>2</sub>), 32.2 (CH<sub>2</sub>-C-(CH<sub>3</sub>)<sub>2</sub>), 27.8 (2 CH<sub>3</sub>); EI-MS,  $m/z$   $[\text{M}]^+$  calcd for  $[\text{C}_{14}\text{H}_{16}\text{N}_2\text{O}_3]^+$ : 260.11, found 260.89; Anal. calcd. for  $\text{C}_{14}\text{H}_{16}\text{N}_2\text{O}_3$ : C, 64.60; H, 6.20; N, 10.76; found C, 64.87; H, 6.00; N, 10.66.

### 2-[(4-Nitrophenyl)carbamoyl]-1,3-dioxo-2,3-dihydro-1H-inden-2-yl 4-(trifluoromethyl)benzoate (**32**)

*p*-Nitrophenyl isocyanide **3** (50 mg, 0.337 mmol), was added to a solution of ninhydrin **31** (59.9 mg, 0.337 mmol), trifluoromethyl benzoic acid (58.3 mg, 0.307 mmol,) in a mixture of 2,2,2-trifluoroethanol (TFE) and ethanol (1:1, 2ml). The mixture was stirred under Reflux for 3 hours. The reaction was monitored by TLC. After the reaction completion, the mixture was cooled to precipitate the desired product then filtered. The product was washed with a saturated solution of NaHCO<sub>3</sub>, then dried and collected without further purification. Yield 46%; white powder; Mp= 210-212°C;  $R_f$  0.75 (EtOAc - petroleum ether, 1:2); IR:  $\nu_{\text{max}}/\text{cm}^{-1}$  3331 (NH), 1733 (CO), 1715 (CO), 1692 (OCN);  $^1\text{H}$  NMR (500 MHz, DMSO- $d_6$ )  $\delta_{\text{H}}$ : 11.42 (s, 1H, NH), 8.42 (d,  $J = 8$  Hz, 2H, Ar-H), 8.25 (d,  $J = 9$  Hz, 2H, Ar-H), 8.21 – 8.19 (m, 2H, Ar-H), 8.17 – 8.15 (m, 2H, Ar-H), 8.03 (d,  $J = 8$  Hz, 2H, Ar-H), 7.96 (d,  $J = 9$  Hz, 2H, Ar-H);  $^{13}\text{C}$  NMR (125 MHz, DMSO- $d_6$ )  $\delta_{\text{C}}$ : 190.7 (2C=O), 163.2 (NH-C=O), 161.5 (O-C=O), 143.7, 143.0, 140.4, 137.6, 131.6, 126.1, 124.7 (Ar-C) 124.3 (CF<sub>3</sub>), 121.3, 112.3 (Ar-C), , 84.7 (O=C-C-O); EI-MS,  $m/z$   $[\text{M}]^+$  calcd for  $[\text{C}_{24}\text{H}_{13}\text{F}_3\text{N}_2\text{O}_7]^+$ : 498.06, found 498.62; Anal. calcd. for  $\text{C}_{24}\text{H}_{13}\text{F}_3\text{N}_2\text{O}_7$ : C, 57.84; H, 2.63; N, 5.62; found C, 57.55; H, 2.53; N, 5.42.

### Procedure for Passerini new products with ninhydrin

A mixture of *p*-nitrophenyl isocyanide **3** (50 mg, 0.337 mmol), ninhydrin (59.9 mg, 0.337 mmol), and trifluoromethyl benzoic acid (**5a**) (58.3 mg, 0.307 mmol) in 2,2,2-trifluoroethanol

(TFE)/ethanol (1:1, 2 mL) was stirred at room temperature for 1 day. The separated product was filtered off, washed with saturated NaHCO<sub>3</sub> solution and dried.

### 2-Ethoxy-2-[(4-nitrophenyl)amino]-1H-indene-1,3(2H)-dione (34)

Yield 70%; off white powder; Mp= 180-183°C; R<sub>f</sub> 0.59 (EtOAc - petroleum ether, 1:2); IR:  $\nu_{\max}/\text{cm}^{-1}$  3350 (NH), 1716 (CO); <sup>1</sup>H NMR (500 MHz, DMSO-*d*<sub>6</sub>)  $\delta_{\text{H}}$ : 8.10 – 8.05 (m, 6H, Ar-H), 8.01 (s, 1H, NH), 7.32 (d, *J* = 9.5 Hz, 2H, Ar-H), 3.74 (q, *J* = 7 Hz, 2H, CH<sub>2</sub>), 1.09 (t, *J* = 7 Hz, 3H, CH<sub>3</sub>); <sup>13</sup>C NMR (125 MHz, DMSO-*d*<sub>6</sub>)  $\delta_{\text{C}}$ : 193.1 (2C=O), 151.1, 138.8, 138.5, 137.8, 125.0, 124.4, 115.5, (Ar-C), 82.7 (NH-C-CO), 59.1 (CH<sub>2</sub>), 14.9 (CH<sub>3</sub>); EI-MS, *m/z* [M]<sup>+</sup> calcd for [C<sub>17</sub>H<sub>14</sub>N<sub>2</sub>O<sub>5</sub>]<sup>+</sup>: 326.09, found 326.25; Anal. calcd. for C<sub>17</sub>H<sub>14</sub>N<sub>2</sub>O<sub>5</sub>: C, 62.57; H, 4.32; N, 8.59; found C, 62.42; H, 4.12; N, 8.65.

### 2-Methoxy-2-[(4-nitrophenyl)amino]-1H-indene-1,3(2H)-dione (35)

Yield 68%; off white powder; Mp= 170-173°C; R<sub>f</sub> 0.57 (EtOAc - petroleum ether, 1:2); IR:  $\nu_{\max}/\text{cm}^{-1}$  3374 (NH), 1705 (CO); <sup>1</sup>H NMR (500 MHz, DMSO-*d*<sub>6</sub>)  $\delta_{\text{H}}$ : 8.10 – 8.05 (m, 6H, Ar-H), 8.03 (bs, 1H, NH), 7.31 (d, *J* = 9 Hz, 2H, Ar-H), 3.42 (s, 3H, CH<sub>3</sub>); <sup>13</sup>C NMR (125 MHz, DMSO-*d*<sub>6</sub>)  $\delta_{\text{C}}$ : 192.9 (2 C=O), 151.1, 138.9, 138.5, 137.8, 125.0, 124.4, 118.9, 115.5, (Ar-C), 82.7 (NH-C-CO), 51.0 (CH<sub>3</sub>); EI-MS, *m/z* [M]<sup>+</sup> calcd for [C<sub>16</sub>H<sub>12</sub>N<sub>2</sub>O<sub>5</sub>]<sup>+</sup>: 312.07, found 312.11; Anal. calcd. for C<sub>16</sub>H<sub>12</sub>N<sub>2</sub>O<sub>5</sub>: C, 61.54; H, 3.87; N, 8.97; found C, 61.25; H, 3.78; N, 8.87.

## 5.2. Anticancer evaluation

### 5.2.1. Cytotoxicity Screening

Normal human lung fibroblast Wi-38 cell line was used to detect cytotoxicity of the studied compounds compared to currently used anticancer drug (doxorubicin). Wi-38 cell line was subcultured in DMEM medium-contained 10% fetal bovine serum (FBS), seeded as 5×10<sup>3</sup> cells per well in 96-well cell culture plate and incubated at 37°C in 5% CO<sub>2</sub> incubator. After 24 h for cell attachment, serial concentrations of these compounds and doxorubicin (Dox) were incubated with Wi-38 cells for 72 h. Cell viability was assayed by MTT method [25]. Twenty microliters of 5 mg/ml MTT (Sigma, USA) was added to each well and the plate was incubated at 37°C for 3 h. Then MTT solution was removed, 100  $\mu$ L DMSO was added and the absorbance of each well was measured with a microplate reader (BMG LabTech, Germany) at 570 nm. The IC<sub>50</sub> and EC<sub>100</sub> values of the tested compounds that cause 50% and 100% cell viability were estimated by the GraphPad InStat software. Anticancer effect of the above-mentioned compounds was assayed using three human cancer cell lines. Breast cancer cell line (MCF-7), liver cancer cell line (HepG-2) and myeloid leukemia cell line (NFS-60) were cultured in RPMI-1640 (Lonza, USA) supplemented with 10% FBS. All cancer cells (5×10<sup>3</sup> cells/ well) were seeded in sterile 96-well plates. After 24h, serial concentrations of the tested compounds and Dox were incubated with three cancer cell lines for 72 h at 37°C in 5% CO<sub>2</sub> incubator. MTT method was done as described above. The half maximal inhibitory concentration (IC<sub>50</sub>) values were calculated using the GraphPad InStat software.

### 5.2.2. Morphological examination of the induced apoptosis

Cellular morphological changes before and after treatment with the most effective and safest anticancer compounds were investigated using phase contrast inverted microscope with a digital camera (Olympus, Japan).

### 5.2.3. Flow cytometric analysis of apoptosis

The IC<sub>50</sub> of the most effective compounds and Dox was incubated for 72 h with MCF-7, NFS-60, and HepG-2 cell lines. After trypsinization, the untreated and treated cells were incubated with annexin V/PI for 15 min., and then cells were fixed and incubated with streptavidin-fluorescein (5 µg/ mL) for 15 min. The apoptosis-dependent anticancer effect was determined by quantification of annexin-stained apoptotic cells using the FITC signal detector (FL1) against the phycoerythrin emission signal detector (FL2).

### 5.2.4. Caspase 3/7 activation assay

The percentage of caspase 3/7 activation was quantified using the Caspase-Glo 3/7 kit following the manufacturer's instructions. This kit used a luminogenic substrate that was cleaved by caspases resulting in the generation of the luminescent signal. This signal was measured by the fluorescence omega microplate reader (BMG LabTech, Germany) at 490 nm excitation and 520 nm emission.

### 5.2.5. Quantification of the apoptosis-inducing factor1 (AIF1)

The level of AIF1 was estimated using ELISA kit (Abcam, United Kingdom) following the manufacturer's protocol. Briefly, extracts of untreated and the most effective anticancer-treated cancer cells were added to anti-AIF1-coated wells following by the incubation for 1 h with horseradish peroxidase-conjugated antibody. Then wells were washed and tetramethylbenzidine (substrate solution) was added. After 10 min, a reaction was stopped by adding stop solution and the wells were measured at 450 nm using spectrophotometer microplate reader (BMG LabTech, Germany).

## 5.3. Antimicrobial evaluation

Selected compounds were evaluated against *Staphylococcus aureus* (ATCC 25923), *Enterococcus faecalis* (ATCC 29212), *Escherichia coli* (ATCC 25922), *Pseudomonas aeruginosa* (ATCC 27853), and *Candida albicans* (ATCC 90028). Their inhibition zones were measured using the agar well diffusion technique [42], and their minimal inhibitory concentrations (MIC) were measured using the broth microdilution assay [43]. Ciprofloxacin was used as a standard antibacterial agent, while fluconazole was used as an antifungal reference. DMSO was used as a blank and showed no antimicrobial activity.

### 5.3.1. Agar well diffusion assay

In the agar well diffusion method [42], 100 µL of suspension containing  $1 \times 10^8$  CFU/mL of pathological tested bacteria and  $1 \times 10^6$  CFU/mL of fungi were spread on nutrient agar. After the media had cooled and solidified, wells (10 mm in diameter) were made in the

solidified agar and loaded with 100  $\mu$ L of the test compound solution; prepared by dissolving in DMSO by final concentration 1mg/mL. The inoculated plates were then incubated for 24 h at 37 °C for bacteria and 48 h at 28 °C for fungi. Negative controls were prepared using DMSO. Ciprofloxacin (1 mg/mL) was used as a standard for antibacterial activity, while Fluconazole (1 mg/mL) was used as a standard for antifungal activity. After incubation time, antimicrobial activity was evaluated by measuring the zones of inhibition in millimeters (mm) against the test organisms and compared with that of the standards.

### 5.3.2. Microdilution assay

In the broth microdilution method [43], two fold serial dilutions of the test compound solutions were prepared using the proper nutrient Mueller Hinton broth. The appropriate inoculums were added and incubated at 37°C for 24 h. The lowest concentration showing no growth was taken as the minimum inhibitory concentration (MIC).

### 5.4. Data analysis and statistics

Data were expressed as mean  $\pm$  standard error of the mean (SEM). Statistical significance was estimated by the multiple comparisons Tukey post-hoc analysis of variance (ANOVA) using the SPSS16 program. The differences were considered statistically significant at  $p < 0.05$ .

## References

- [1] Cancer, <http://www.who.int/news-room/fact-sheets/detail/cancer> (accessed January 13, 2019).
- [2] L.A. Torre, F. Bray, R.L. Siegel, J. Ferlay, J. Lortet-Tieulent, A. Jemal, Global cancer statistics, 2012, CA. Cancer J. Clin. 65 (2015) 87–108. doi:10.3322/caac.21262.
- [3] G.M. Cooper, Cell proliferation in development and differentiation, Cell A Mol. Approach. 2nd Ed. Sunderl. Sinauer Assoc. (2000).
- [4] H. Calvert, Cancer Drug Design and Discovery, in: S.B.T.-C.D.D. and D. (Second E. Neidle (Ed.), Academic Press, San Diego, 2014: pp. xi–xiii. doi 10.1016/B978-0-12-396521-9.06001-0.
- [5] J.C. Reed, Dysregulation of apoptosis in cancer, J. Clin. Oncol. 17 (1999) 2941–2953. doi:10.1200/JCO.1999.17.9.2941.
- [6] R.S. Wong, Apoptosis in cancer: from pathogenesis to treatment, J. Exp. Clin. Cancer Res. 30 (2011) 1–87. doi:10.1186/1756-9966-30-87.
- [7] J.C. Reed, K.J. Tomaselli, Drug discovery opportunities from apoptosis research, Curr. Opin. Biotechnol. 11 (2000) 586–592. doi:10.1016/S0958-1669(00)00148-8.
- [8] D. Leung, G. Abbenante, D.P. Fairlie, Protease inhibitors: current status and future prospects, J. Med. Chem. 43 (2000) 305–341. doi:10.1021/jm990412m.
- [9] D. Nicholson, Caspase structure, proteolytic substrates and function during apoptotic cell death, Cell Death Differ. 6 (1999) 1028–1042. doi:10.1038/sj.cdd.4400598.
- [10] N.A. Thornberry, Caspases: Key mediators of apoptosis, Chem. Biol. 5 (1998) R97–R103. doi:10.1016/S1074-5521(98)90615-9.
- [11] A.G. Porter, R.U. Jänicke, Emerging roles of caspase-3 in apoptosis, Cell Death Differ. 6 (1999) 99–104. doi:10.1038/sj.cdd.4400476.
- [12] A. Clark, S. MacKenzie, Targeting Cell Death in Tumors by Activating Caspases, Curr. Cancer Drug Targets. 8 (2008) 98–109. doi:10.2174/156800908783769391.
- [13] H. Liang, R.A. Salinas, B.Z. Leal, T. Kosakowska-Cholody, C.J. Michejda, S.J. Waters, T.S. Herman, J.M. Woynarowski, B.A. Woynarowska, Caspase-mediated apoptosis and caspase-independent cell death induced by irifolven in prostate cancer cells, in: Mol. Cancer Ther., 2004: p. 1385 LP-1396.

- [14] X. Jiang, H.E. Kim, H. Shu, Y. Zhao, H. Zhang, J. Kofron, J. Donnelly, D. Burns, S. chung Ng, S. Rosenberg, X. Wang, Distinctive roles of PHAP proteins and prothymosin- $\alpha$  in a death regulatory pathway, *Science* (80-. ). 299 (2003) 223–226. doi:10.1126/science.1076807.
- [15] I. Weber, B. Fang, J. Agniswamy, Caspases: Structure-Guided Design of Drugs to Control Cell Death, *Mini-Reviews Med. Chem.* 8 (2008) 1154–1162. doi:10.2174/138955708785909899.
- [16] S.X. Cai, B. Nguyen, S. Jia, J. Herich, J. Guastella, S. Reddy, B. Tseng, J. Drewe, S. Kasibhatla, Discovery of Substituted N -Phenyl Nicotinamides as Potent Inducers of Apoptosis Using a Cell- and Caspase-Based High Throughput Screening Assay, *J. Med. Chem.* 46 (2003) 2474–2481. doi:10.1021/jm0205200.
- [17] C. Du, M. Fang, Y. Li, L. Li, X. Wang, Smac, a Mitochondrial Protein that Promotes Cytochrome c-Dependent Caspase Activation by Eliminating IAP Inhibition, *Cell.* 102 (2000) 33–42. doi:10.1016/S0092-8674(00)00008-8.
- [18] J. Chai, C. Du, J.W. Wu, S. Kyin, X. Wang, Y. Shi, Structural and biochemical basis of apoptotic activation by Smac/DIABLO, *Nature.* 406 (2000) 855–862. doi:10.1038/35022514.
- [19] T.K. Oost, C. Sun, R.C. Armstrong, A.S. Al-Assaad, S.F. Betz, T.L. Deckwerth, H. Ding, S.W. Elmore, R.P. Meadows, E.T. Olejniczak, A. Oleksijew, T. Oltersdorf, S.H. Rosenberg, A.R. Shoemaker, K.J. Tomaselli, H. Zou, S.W. Fesik, Discovery of potent antagonists of the antiapoptotic protein XIAP for the treatment of cancer, *J. Med. Chem.* 47 (2004) 4417–4426. doi:10.1021/jm040037k.
- [20] L. Bai, D.C. Smith, S. Wang, Small-molecule SMAC mimetics as new cancer therapeutics, *Pharmacol. Ther.* 144 (2014) 82–95. doi:10.1016/j.pharmthera.2014.05.007.
- [21] H. Sun, Z. Nikolovska-Coleska, C.-Y. Yang, D. Qian, J. Lu, S. Qiu, L. Bai, Y. Peng, Q. Cai, S. Wang, Design of Small-Molecule Peptidic and Nonpeptidic Smac Mimetics, *Acc. Chem. Res.* 41 (2008) 1264–1277. doi:10.1021/ar8000553.
- [22] C.N. Johnson, J.S. Ahn, I.M. Buck, E. Chiarparin, J.E.H. Day, A. Hopkins, S. Howard, E.J. Lewis, V. Martins, A. Millemaggi, J.M. Munck, L.W. Page, T. Peakman, M. Reader, S.J. Rich, G. Saxty, T. Smyth, N.T. Thompson, G.A. Ward, P.A. Williams, N.E. Wilsher, G. Chessari, A Fragment-Derived Clinical Candidate for Antagonism of X-Linked and Cellular Inhibitor of Apoptosis Proteins: 1-(6-[(4-Fluorophenyl)methyl]-5-(hydroxymethyl)-3,3-dimethyl-1 H,2 H,3 H-pyrrolo[3,2- b]pyridin-1-yl)-2-[(2 R,5 R)-5-methyl-2-[(3R)-3-methylmor, *J. Med. Chem.* 61 (2018) 7314–7329. doi:10.1021/acs.jmedchem.8b00900.
- [23] A. Reza Kazemizadeh, A. Ramazani, Synthetic Applications of Passerini Reaction, *Curr. Org. Chem.* 16 (2012) 418–450. doi:10.2174/138527212799499868.
- [24] M. Zeller, A.D. Hunter, p -Nitrophenyl isocyanide, *Acta Crystallogr. Sect. C Cryst. Struct. Commun.* 60 (2004) o415–o417. doi:10.1107/S0108270104007115.
- [25] T. Mosmann, Rapid colorimetric assay for cellular growth and survival: Application to proliferation and cytotoxicity assays, *J. Immunol. Methods.* 65 (1983) 55–63. doi:10.1016/0022-1759(83)90303-4.
- [26] M.R. Felício, O.N. Silva, S. Gonçalves, N.C. Santos, O.L. Franco, Peptides with Dual Antimicrobial and Anticancer Activities, *Front. Chem.* 5 (2017) 5–5. doi:10.3389/fchem.2017.00005.
- [27] J.-G. Kim, D. Jang, Facile and Highly Efficient N-Formylation of Amines Using a Catalytic Amount of Iodine under Solvent-Free Conditions, *Synlett.* 2010 (2010) 2093–2096. doi:10.1055/s-0030-1258518.
- [28] R. Obrecht, R. Herrmann, I. Ugi, Isocyanide Synthesis with Phosphoryl Chloride and Diisopropylamine, *Synthesis (Stuttg).* 1985 (1985) 400–402. doi:10.1055/s-1985-31216.
- [29] S. Berłozeki, W. Szymanski, R. Ostaszewski,  $\alpha$ -Amino acids as acid components in the Passerini reaction: influence of N-protection on the yield and stereoselectivity, *Tetrahedron.* 64 (2008) 9780–9783. doi:10.1016/j.tet.2008.07.064.
- [30] M.J. Thompson, B. Chen, Ugi reactions with ammonia offer rapid access to a wide range of 5-aminothiazole and oxazole derivatives, *J. Org. Chem.* 74 (2009) 7084–7093. doi:10.1021/jo9014529.
- [31] J. Zakrzewski, J. Jezierska, J. Hupko, 4-Isocyano-2,2,6,6-tetramethylpiperidin- 1-oxyl: A Valuable Precursor for the Synthesis of New Nitroxides, *Org. Lett.* 6 (2004) 695–697. doi:10.1021/ol036298q.

- [32] I. Lengyel, V. Cesare, T. Taldone, A direct link between the Passerini reaction and  $\alpha$ -lactams, *Tetrahedron*. 60 (2004) 1107–1124. doi:10.1016/j.tet.2003.11.067.
- [33] J.E. Semple, T.D. Owens, K. Nguyen, O.E. Levy, New Synthetic Technology for Efficient Construction of  $\alpha$ -Hydroxy- $\beta$ -amino Amides via the Passerini Reaction 1, *Org. Lett.* 2 (2000) 2769–2772. doi:10.1021/ol0061485.
- [34] L. El Kaim, L. Grimaud, Beyond the Ugi reaction: less conventional interactions between isocyanides and iminium species, *Tetrahedron*. 65 (2009) 2153–2171. doi:10.1016/j.tet.2008.12.002.
- [35] S. Erol Gunal, S. Teke Tuncel, N. Gokhan Kelekci, G. Ucar, B. Yuce Dursun, S. Sag Erdem, I. Dogan, Asymmetric synthesis, molecular modeling and biological evaluation of 5-methyl-3-aryloxazolidine-2,4-dione enantiomers as monoamine oxidase (MAO) inhibitors, *Bioorg. Chem.* 77 (2018) 608–618. doi:10.1016/j.bioorg.2018.02.003.
- [36] S.D. Edmondson, A. Mastracchio, E.R. Parmee, Palladium-Catalyzed Coupling of Vinylogous Amides with Aryl Halides: Applications to the Synthesis of Heterocycles, *Org. Lett.* 2 (2000) 1109–1112. doi:10.1021/ol000031z.
- [37] A.R. Karimi, A. Rajabi-Khorrami, Z. Alimohammadi, A.A. Mohammadi, M.R. Mohammadizadeh, Three-Component Synthesis of Ninhydrin Derived  $\alpha$ -Acylloxycarboxamides, *Monatshefte Für Chemie - Chem. Mon.* 137 (2006) 1079–1082. doi:10.1007/s00706-006-0501-5.
- [38] N.A.M. Akhir, L.S. Chua, F.A.A. Majid, M.R. Sarmidi, Cytotoxicity of Aqueous and Ethanolic Extracts of *Ficus deltoidea* on Human Ovarian Carcinoma Cell Line, *Br. J. Med. Med. Res.* 1 (2011) 397–409. doi:10.9734/BJMMR/2011/507.
- [39] A.P.-S.A.F.Z.B.E. V. SILANO, Toxicity tests with mammalian cell cultures, in: *Short-Term Toxic. Tests Non-Genotoxic Eff.*, 2nd Editio, 1990: pp. 75–97.
- [40] Y. Cao, R.A. Depinho, M. Ernst, K. Vousden, Cancer research: Past, present and future, *Nat. Rev. Cancer.* 11 (2011) 749–754. doi:10.1038/nrc3138.
- [41] P. Prayong, S. Barusux, N. Weerapreeyakul, Cytotoxic activity screening of some indigenous Thai plants, *Fitoterapia*. 79 (2008) 598–601. doi:10.1016/j.fitote.2008.06.007.
- [42] C. Perez, M. Pauli, P. Bazerque, Antibiotic assay by Agar well diffusion method, *Acta. Biol. Med. Exp.* 15 (1990) 113–115.
- [43] P. da S. Nascente, A.R.M. Meinerz, R.O. De Faria, L.F.D. Schuch, M.C.A. Meireles, J.R.B. de Mello, CLSI broth microdilution method for testing susceptibility of *Malasseziapachydermatis* to thiabendazole, *Brazilian J. Microbiol.* 40 (2009) 222–226. doi:10.1590/S1517-83822009000200002.
- [44] Molinspiration cheminformatics., <https://www.molinspiration.com/> (accessed January 13, 2019).
- [45] C.A. Lipinski, F. Lombardo, B.W. Dominy, P.J. Feeney, Experimental and computational approaches to estimate solubility and permeability in drug discovery and development settings 1PII of original article: S0169-409X(96)00423-1. The article was originally published in *Advanced Drug Delivery Reviews* 23 (1997) , *Adv. Drug Deliv. Rev.* 46 (2001) 3–26. doi:10.1016/S0169-409X(00)00129-0.
- [46] D.F. Veber, S.R. Johnson, H.-Y. Cheng, B.R. Smith, K.W. Ward, K.D. Kopple, Molecular Properties That Influence the Oral Bioavailability of Drug Candidates, *J. Med. Chem.* 45 (2002) 2615–2623. doi:10.1021/jm020017n.
- [47] P. Ertl, B. Rohde, P. Selzer, Fast calculation of molecular polar surface area as a sum of fragment-based contributions and its application to the prediction of drug transport properties, *J. Med. Chem.* 43 (2000) 3714–3717. doi:10.1021/jm000942e.
- [48] A. Polinsky, HIGH-SPEED CHEMISTRY LIBRARIES: ASSESSMENT OF DRUG-LIKENESS, in: *Pract. Med. Chem.*, Elsevier, 2003: pp. 147–157. doi:10.1016/B978-012744481-9/50014-3.
- [49] Molsoft L.L.C.: Drug-Likeness and molecular property prediction., <http://molsoft.com/mprop/> (accessed January 13, 2019).
- [50] M.A. Bakht, M.S. Yar, S.G. Abdel-Hamid, S.I. Al Qasoumi, A. Samad, Molecular properties prediction, synthesis and antimicrobial activity of some newer oxadiazole derivatives, *Eur. J. Med. Chem.* 45 (2010) 5862–5869. doi:10.1016/j.ejmech.2010.07.069.
- [51] C.H. Reynolds, B.A. Tounge, S.D. Bembenek, Ligand Binding Efficiency: Trends, Physical Basis, and Implications, *J. Med. Chem.* 51 (2008) 2432–2438. doi:10.1021/jm701255b.
- [52] P.R. Andrews, D.J. Craik, J.L. Martin, Functional Group Contributions to Drug-Receptor

- Interactions, *J. Med. Chem.* 27 (1984) 1648–1657. doi:10.1021/jm00378a021.
- [53] M. Orita, K. Ohno, M. Warizaya, Y. Amano, T. Niimi, Lead Generation and examples: Opinion regarding how to follow up hits, *Methods Enzymol.* 493 (2011) 383–419. doi:10.1016/B978-0-12-381274-2.00015-7.
- [54] H. Chen, O. Engkvist, T. Kogej, Compound Properties and Their Influence on Drug Quality, in: *Pract. Med. Chem. Fourth Ed.*, Elsevier, 2015: pp. 379–393. doi:10.1016/B978-0-12-417205-0.00015-8.
- [55] G.M. Keserü, G.M. Makara, The influence of lead discovery strategies on the properties of drug candidates, *Nat. Rev. Drug Discov.* 8 (2009) 203–212. doi:10.1038/nrd2796.
- [56] I. Jabeen, K. Pleban, U. Rinner, P. Chiba, G.F. Ecker, Structure-activity relationships, ligand efficiency, and lipophilic efficiency profiles of benzophenone-type inhibitors of the multidrug transporter P-glycoprotein, *J. Med. Chem.* 55 (2012) 3261–3273. doi:10.1021/jm201705f.
- [57] S.L. Planey, R. Kumar, Lipophilicity indices for drug development, *J. Appl. Biopharm. Pharmacokinet.* 1 (2013) 31–36. doi:10.14205/2309-4435.2013.01.01.6.
- [58] N.E. Dixon, P.W. Riddles, C. Gazzola, R.L. Blakeley, B. Zerner, Jack bean urease (EC 3.5.1.5). V. On the mechanism of action of urease on urea, formamide, acetamide, N -methylurea, and related compounds, *Can. J. Biochem.* 58 (1980) 1335–1344. doi:10.1139/o80-181.
- [59] I. Ugi, U. Fetzer, U. Eholzer, H. Knupfer, K. Offermann, Isonitrile Syntheses, *Angew. Chemie Int. Ed. English.* 4 (1965) 472–484. doi:10.1002/anie.196504721.
- [60] Z.N. Siddiqui, K. Khan, N. Ahmed, Nano fibrous silica sulphuric acid as an efficient catalyst for the synthesis of  $\beta$ -enaminone, *Catal. Letters.* 144 (2014) 623–632. doi:10.1007/s10562-013-1190-4.

**Highlights**

- Cytotoxicity of newly synthesized Passerini compounds was evaluated.
- Compounds **13** and **21** exhibited more potent caspase-dependent apoptotic induction than doxorubicin.
- Selected compounds were screened for dual anticancer/antimicrobial activities.
- *In silico* drug-likeness data were predicted for all compounds.